Proceedings of the National Conference on

Current Trends and Future Extensions of Green Chemistry (CTFEGC)

Exploring the Structures and Properties of Advance Materials and Molecules

Sponsored by

Council of Scientific & Industrial Research

Editors

Dr. Avishek Ghosh
Dr. Jagannath Pal
Dr. Prankrishna Manna
Dr. Manisha Das

Organised by

MIDNAPORE CITY COLLEGE
(Recognised by UGC, Govt of India & Affiliated to Vidyasagar Universty)
Midnapore, Paschim Medinipur, Pin- 721129, West Bengal, India
wwww.mcconline.org.in | director@mcconline.org.in

Proceedings of the National Conference on

Current Trends and Future Extensions of Green Chemistry (CTFEGC)

Exploring the Structures and Properties of Advance Materials and Molecules

Sponsored by

Council of Scientific & Industrial Research

Editors

Dr. Avishek Ghosh
Dr. Jagannath Pal
Dr. Prankrishna Manna
Dr. Manisha Das

Organised by

MIDNAPORE CITY COLLEGE

(Recognised by UGC, Govt of India & Affiliated to Vidyasagar Universty)
Midnapore, Paschim Medinipur, Pin- 721129, West Bengal, India
wwww.mcconline.org.in | director@mcconline.org.in

Proceedings of the National Conference on Current Trends and Future Extensions of Green Chemistry (CTFEGC):
Exploring the Structures and Properties of Advance Materials and Molecules
Edited by Dr. Avishek Ghosh, Dr. Jagannath Pal, Dr. Prankrishna Manna &
Dr. Manisha Das

First Published: 2023

Co-Published by
Midnapore City College
Department of Chemistry
Paschim Medinipur, West Bengal, India
&
Levant Books
27C Creek Row,
Kolkata 700 014, India

ISBN: 978-00-00000-00-0

Printed and bound at
Sarat Impressions Pvt. Ltd**.**
18B, Shyama Charan Dey Street,
Kolkata - 700 073

Preface

This Proceedings aims at serving educators for expressing their views on Current trends and future extensions of green chemistry. Since about the 1990s, "green" has come into widespread use as a term to describe practices and disciplines that deal with sustainability and the maintenance of environmental quality. Most works on green chemistry have concentrated on aspects of chemical synthesis, especially organic chemical synthesis. Current trends and future extensions of green chemistry discusses chemistry as a whole particularly as it relates to the environment and sustainability.

The Volume contains a collection of papers presented at the conference on Current Trends and Future Extensions of Green Chemistry (CTFEGC-23) organized by Department of Chemistry, Midnapore City College and sponsored by Council of Scientific & Industrial Research (CSIR) held on 21st-22nd September, 2023, where many Researchers, Teaching Faculties participated and presented their research along with a platform of 200 undergraduate and post graduate students of allied disciplines. The eminent scientists of India delivered their talk based on green chemistry. The main objective of this conference are to identify new approaches and research opportunities in green chemistry and their usefulness in future which link different disciplines of research areas and boosting the research activities in college.

We express our heartiest gratitude to all faculty members, academic personalities and stuff whose unconditional efforts make possible during preparation of this volume of Proceedings and associated works of the symposium. We thank all the authors for submitting their research work. The financial assistance made by CSIR, India is highly acknowledged.

Contents

AN INSIGHT INTO THE RARELY FOUND NONOXIDO VANADIUM (IV) COMPLEXES

Dr. Subhashree P. Dash
Parala Maharaja Engineering College, Berhampur, 761003, Odisha

Vanadium plays a number of roles in biological systems and has been found in many naturally occurring compounds.[1] In humans, V compounds exhibit a wide variety of pharmacological properties, and many complexes have been tested as antiparasitic, spermicidal, antiviral, anti-HIV, antituberculosis, and antitumor agents.[2] Particularly, vanadium has been proven to be one of the most efficient metal ions with potential antidiabetic activity.[3] Vanadium complexes show varied stereochemistry. It can form compounds with inorganic and organic ligands, with a particular preference for oxygen, nitrogen, and sulphur donor atoms.

Again, the coordination chemistry of variable valence vanadium assumed special importance due to the following reasons:

1. Vanadium in higher oxidation states (+5 and +4) is oxidophilic. It forms various types of oxido species depending on the charge and denticity of the coordinating ligand attached to the metal centers.[4] Among these compounds, those containing the VO^{n+} (n = 2−3) and $[V_2O_3]^{n+}$ (n = 2−4) cores belong to the largest family.

2. Many oxidation states of vanadium are relevant for biological systems like +III, +IV, and +V.[5,6] However, V^{III} is very susceptible to oxidation and appears to be of less importance than V^{IV} and V^{V}.
3. Although the chemistry of oxido vanadium (IV) and (V) complexes is well developed, the number of nonoxido vanadium (IV) complexes in the electronic Cambridge Structural Database remains scarce. Formation of nonoxido or 'bare' hexacoordinated vanadium (IV) complexes is rather difficult because the strong V=O bond must be broken and the oxido ligand must leave the complex as a good leaving group.

In this context, the chemistry of non-oxidovanadium (IV) with ligands of various types has been of significant importance in this regard. Review on some of the recent reports of the nonoxido vanadium (IV) complexes with O- and N- donor environments, which are drawing much current attention, are highlighted below

Nonoxido vanadium (IV) complexes. Vanadium is an oxidophilic metal and tends to form oxido-species in its +5 and +4 oxidation states. But certain vanadium complexes contain no oxido group and are known to be nonoxido or 'bare' complexes. In recent times such species have attracted special attention from inorganic chemists due to their structural similarities with amavadin. Amavadin is the first octacoordinated

vanadium (IV) complex isolated from Amanita mushrooms.[7,8] It is a nonoxido vanadium (IV) complex but this character was established after a long time.[9,10] Three types of nonoxido vanadium (IV) compounds, viz. hexa-, hepta-, and octacoordinate, are reported. A characteristic feature of all nonoxido vanadium (IV) complexes is the absence of the (V=O) band in the 935–1035 cm^{-1} region in the IR spectra, which, in contrast, is a signature for all oxido vanadium (IV) and (V) compounds. P. Chaudhuri[11] and the group have contributed a lot in the field of nonoxido vanadium chemistry. In 2011 they reported the structural and magnetochemical characterization of two nonoxido vanadium (IV) complexes [$LV^{IV}(OCH_3)$] (**1**) (**Figure 1**) and [LV^{IV}(acac)] (**2**) using tris(2-hydroxy-3,5-di-*tert* butylbenzyl) amine as ligand (H_3L).

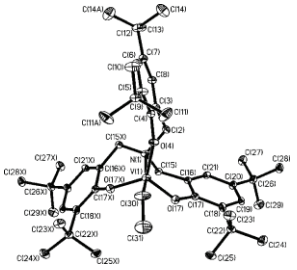

Figure 1

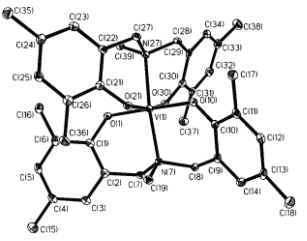

Figure 2

In 2004, the same group[12] reported, another series of nonoxido vanadium (IV) complexes taking potentially tridentate bisphenol ligands (H_2L). In 2003, Chaudhuri et al.[13] also reported two mononuclear nonoxido vanadium (IV) complexes, [$V^{IV}LMe_2$] (**3**) (**Figure 2**) and [$V^{IV}Lt Bu_2$] (**4**), with a tridentate bis(phenol) ligand (H_2L) bearing the O_2N donor atoms and with either dimethyl or di*tert*-butyl substituents. Ghosh et al.[14] have reported a very general route for the synthesis of a series of stable octacoordinated nonoxido vanadium (IV) complexes of the general formula VL_2 (where H_2L is an ONNO donor tetradentate hydrazone ligand). These compounds were found to be highly stable in open air, in the solid state as well as in solution and don't require any inert condition for synthesis, which is an unusual phenomenon for such types of complexes. One of these compounds $VL^1{}_2$ (**5**) has been structurally characterized (**Figure 3**) {where H_2L^1 = benzildihydrazone of 2-aminobenzoylhydrazine} and was found to exhibit a dodecahedral structure existing in a tetragonal space group $P\bar{4}n2$ Garribba et al.[15] have reported the synthesis and characterization of two nonoxido vanadium(IV) complexes, [$V(H_{-3}ino)_2$][$K_2(ino)_2$].$4H_2O$ (**6**) and [$Na_6V(H_{-3}ino)_2$](SO_4)$_2$.$6H_2O$ (**7**) {where, ino = cis-inositol}. Structures of both the complexes were determined by single-crystal X-ray analysis. Crystal structure of the **6** (**Figure 4**) represents an unusual 1:1 packing of $[V(H_{-3}ino)_2]^{2-}$ dianions and $[K_2(ino)_2]^{2+}$ dications, in which both K^+ ions have a coordination number of nine and are bonded simultaneously to a 1,3,5-triaxial and a 1,2,3-axial-equatorial-axial site of ino. Dinda et al[16] has also reported the synthesis and characterization of two nonoxido vanadium (IV) complexes along with their biological application such as insulin mimetic and antiproliferative activities

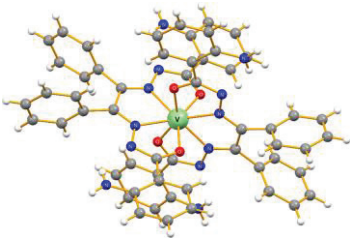

Figure 3

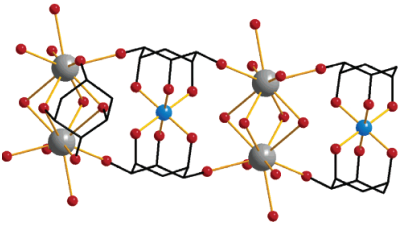

Figure 4

References:

1. (a) Crans DC, Smee JJ, Gaidamauskas E, Yang L. The Chemistry and Biochemistry of Vanadium and the Biological Activities Exerted by Vanadium Compounds. Chem. Rev. **2004**, 104, 849–902. (b) Rehder D, Bioinorganic Vanadium Chemistry; John Wiley & Sons Ltd.: Chichester, **2008**.

2. (a) Rehder D. Future Med. Chem. **2012**, 4, 1823. (b) Pessoa J C, Tomaz I. Curr. Med. Chem. **2010**, 17, 3701.

3. (a) Thompson KH, Orvig C. Coordination chemistry of vanadium in metallopharmaceutical candidate compounds. Coord. Chem. Rev. **2001**, 219−221, 1033. (b) Sakurai H, Yoshikawa Y, Yasui H. Current state for the development of metallopharmaceutics and anti-diabetic metal complexes. Chem. Soc. Rev. **2008**, 37, 2383-2392.

4. The Seventh International Symposium on the Chemistry and Biological Chemistry of Vanadium. In Coordination Chemistry Reviews, Michibata H, Kanamori K, Hirao T, Eds. Elsevier BV: Amsterdam, The Netherlands, **2011**, 255, 2149.

5. Rehder D. Bioinorganic Vanadium Chemistry. John Wiley & Sons, Ltd: Chichester, U. K. **2008**, 1.

6. Crans DC, Smee JJ, Gaidamauskas E, Yang L. The Chemistry and Biochemistry of Vanadium and the Biological Activities Exerted by Vanadium Compounds. Chem. Rev. **2004**, 104, 849–902.

7. Bayer E, Kneifel HZ. Isolation of amavadin, a vanadium compound occuring in Amanita muscaria. Naturforsch **1972**, 27B, 207.

8. Kneifel H, Bayer E. Determination of the strucutre of the vanadium compound, amavadin, from fly agaric. Angew. Chem. Int. Ed. Engl. **1973**, 12, 508.

9. de MAAF, Carrondo CT, Duarte MTLS, Pessoa JC, Silva JAL, Fraustoda Silva JJR, Vaz MCTA Vilas-Boas LFJ. Bis-(N-hydroxy-iminodiacetate)vanadate(IV), a synthetic model of 'amavadin'. Chem. Commun. **1988**, 1158-1159.

10. Armstrong EM, Beddoes RL, Calviou LJ, Charnock JM, Collison D, Ertok N, Naismith JH, Garner CD. The chemical nature of amavadin. J. Am. Chem. Soc. **1993**, 115, 807–808.

11. Kajiwara T, Wagner R, Bill E, Weyhermüller T, Chaudhuri P. Non-oxo 5-coordinate and 6-coordinate vanadium(iv) complexes with their precursor $[LV^{III}(CH3OH)]^0$, where L = a trianionic aminetris(phenolate)-[N,O,O,O] donor ligand: a magnetostructural and EPR study. Dalton Trans. **2011**, 40, 12719-12726.

12. Paine T K, Weyhermüller T, Slep L D, Neese F, Bill E, Bothe E, Wieghardt K, Chaudhuri P. Nonoxovanadium(IV) and Oxovanadium(V) Complexes with Mixed O, X, O-Donor Ligands (X = S, Se, P, or PO). Inorg. Chem. **2004**, 43, 7324–7338.

13. Paine TK, Weyhermueller T, Bill E, Bothe E, Chaudhuri P. Non-Oxo Vanadium(IV) Complexes of Aminebis(phenolate) [O,N,O] Donor Ligands and Solution Studies of Isostructural V(IV) and Mn(IV) Complexes. Eur. J. Inorg.Chem. **2003**, 4299-4307.

14. Sutradhar M, Mukherjee G, Drew MGB, Ghosh S. Simple General Method of Generating Non-oxo, Non-amavadine Model Octacoordinated Vanadium(IV) Complexes of Some Tetradentate ONNO Chelating Ligands from Various Oxovanadium(IV/V) Compounds and Structural Characterization of One of Them. Inorg. Chem. **2007**, 46, 5069–5075.

15. Morgenstern B, Kutzky B, Neis C, Stucky S, Hegetschweiler K, Garribba E, Micera G. Synthesis and Characterization of Vanadium(IV) Complexes with cis-Inositol in Aqueous Solution and in the Solid-State. Inorg. Chem. **2007**, 46, 3903–3915.

16. (a). Banerjee A, Dash SP, Mohanty M, Sahu G, Sciortino G, Garribba E, Carvalho FFNN, Marques F, Pessoa JC, Kaminsky W, Brzezinski K, Dinda R. New V^{IV}, $V^{IV}O$, $V^{V}O$, and $V^{V}O_2$ Systems: Exploring their Interconversion in Solution, Protein Interactions, and Cytotoxicity. Inorg. Chem. 2020, 59, 19, 14042−14057. (b) Dash SP, Pasayat S, Bhakat S, Roy S, Dinda R, Tiekink ERT, Mukhopadhyay S, Bhutia SK, Hardikar MR, Joshi BN, Patil YP, Nethaji M Highly stable hexacoordinated nonoxidovanadium(IV) complexes of sterically constrained ligands: syntheses, structure, and study of antiproliferative and insulin mimetic activity. Inorg. Chem. 2013, 52, 14096−14107. (c) Dash SP, Majumder S, Banerjee A, Carvalho MFNN, Adao P, Pessoa, JC, Brzezinski K, Garribba, E, Reuter H, Dinda R. Chemistry of Monomeric and Dinuclear Non-Oxido Vanadium(IV) and Oxidovanadium(V) Aroylazine Complexes: Exploring Solution Behavior. Inorg. Chem. 2016, 55, 1165−1182

SEMI FLUORINATED POLYAMIDE/HOLEY GRAPHENE OXIDE MIXED MATRIX MEMBRANES FOR GAS TRANSPORT PROPERTIES

Barun Kumar Mondal, Soumendu Bisoi*
Narajole Raj College, Department of Chemistry, Vill+PO: Narajole, Paschim Medinipore, PIN : 721211
Corresponding Author e-mail: soumendubisoi@gmail.com

Abstract

Semi fluorinated Polyamide (PA)/holey graphene oxide (HGO) mixed matrix membranes (MMMs) have been prepared and their gas separation performance of four different gases CH_4, N_2, O_2 and CO_2 were measured for the pure and MMMs using a constant-volume variable pressure method. The prepared hybrid PA/holey GO membranes exhibit higher CO_2 permeability and CO_2/CH_4 selectivity than the pure polymer membrane. The most significant improvement is observed for MMMs using 10% of (PA)-functionalized holey GO nanofillers and MMMs are capable of maintaining good CO_2 permeability.

Keywords: Poly(amide), Mixed-Matrix Membranes, Gas permeability, Holey Graphene Oxide.

Introduction:

Current gas separation membrane technologies through polymeric membranes are cost and energy-effective, environmentally benign, as well as simple and versatile. This is due to the attractive combination of low costs with facile processing and innovation that characterizes polymer materials.[1,2] Polyamide membranes attracted substantial attention due to their higher CO_2 permeability and CO_2/CH_4 selectivity at laboratory scale, as compared to cellulose acetate membranes. Over the last two decades, inorganic particles e.g. zeolite and inorganic oxides have been used to prepare mixed-matrix membranes (MMMs), also called hybrid membranes[1,2]. Graphene-based nanofillers hold a clear advantage over other type of fillers. The incorporation of nanopores in graphene oxide (GO) has been proven to increase the diffusivity of MMMs made with other polymers than PA, with pores acting as “open gates” for the transport of gases through the polymer sieve. In order to achieve a good dispersion in the polymer matrix, GO has been functionalized 5-10 wt % of filler (HGO). The prepared MMMs have been tested for single gas permeation tests (CH_4, N_2, O_2, and CO_2) separations. An attempt has been made to understand the structure-property correlations of the MMMs and the role of the graphene-like nanofillers on the final gas permeability.

2. Experimental

2.1. Materials, Membrane Characterization & Gas Separation Measurements

Synthesis of 2,6-bis[3'-trifluoromethyl-4'(4"-carboxyphenoxy)benzyl]pyridine (2) has been reported earlier[4].

2.2. Polymerization

The aromatic diamine (1) was reacted with dicarboxylic acid monomer (2) in molar ratio of 1:1 using NMP as solvent and in the presence of triphenyl phosphite (TPP), $CaCl_2$ and pyridine as shown in **Scheme 1.** The off-white fibrous polymer was dried overnight at 80 °C under vacuum[4].

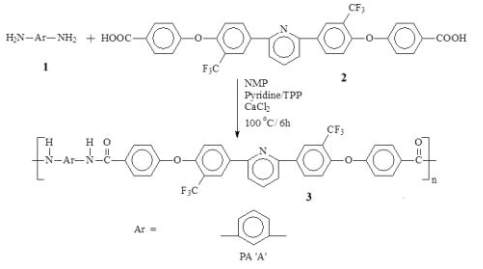

Scheme 1. Synthesis of the poly(amide)s (PA 'A')[1].

2.3. Synthesis of Graphene Oxide (GO) and Holey GO.

In-plane porosity at nanoscale was created on the GO via treatment with an oxidizing agent. 95 mL of an aqueous GO solution (1 mg mL^{-1}) was mixed with 5 mL of H_2O_2 (30 wt %) in a round-bottom flask and left under stirring at 100 °C for 4 h. The product denoted as HGO-4h. 8 h and maintaining the temperature at 100 °C was denoted as HGO-8h.

2.4. Polymeric Membrane Preparation

The membrane was prepared by casting 10-15% (w/v) homogeneous polymer solution in DMF solvent onto clean glass Petri dishes. Free standing flexible membrane were obtained for all the polymer varying thickness from 60-80 μm.

2.5. MMM Membrane preparation

MMMs were prepared by a blending method where the holey GO nanofillers were first dispersed in DMF at 5 and 10 wt % holey GO, the corresponding amount of holey GO were dispersed in DMF. The solution was stirred for 1d and then graphene dispersion was then mixed with a PA A solution in DMF so as to have a final concentration of polymer of 5 wt % & 10 wt %. The solution was cast on a flat-bottom Petri dish, maintaining a ratio of 1 ml solution/1 cm diameter of Petri dish. The inner diameter of the petri dish was 10 cm. oven heated at 80 °C overnight, followed by slow heating to 150 °C and then kept for 6h. The dry film was removed by immersing in a solution of H_2O/IPA (1:1) and then dried in an oven. The film was

heated to 200 ºC at a rate of 20 ºC/h. The membrane was further dried for 8 h at 200 ºC[1].

3. Results and discussion

3.1. Polymer synthesis and their properties

Polyamide was synthesized by the typical phosphorylation polycondensation of the dicarboxylic acid monomer (2) with aromatic diamine monomer (1) (**Scheme 1**). Polymer repeat unit structures were confirmed by elemental analyses, FTIR-ATR and NMR spectroscopic methods.

Synthesized GO formed nanoholes by chemical etching using H_2O_2 as oxidizing agent. XPS was employed to investigate the GO, the materials resulting from its oxidation (HGO-4h and HGO-8h). XPS spectra shows noticeable decrease in the intensity of the C-O and C=O peaks. However, both HGO-4h and HGO-8h show a significant decrease in the peak corresponding to C-O and a small increase in that associated with C=O groups.

TEM images for GO, HGO-4h, and HGO-8h were acquired to study the pore formation process, the influence of the reaction time, and the effect of the oxidizing agent. Both GO (Figure 1a) and HGO-4h (Figure b and c) display homogeneous surfaces with the absence of pores.

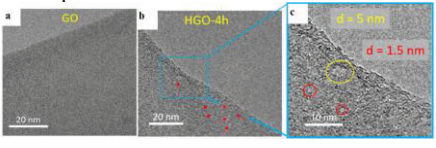

Figure 1. TEM images of GO (a) and at high magnification and HGO-4h (b and c) at high magnification.

The morphologies of pure PA A and MMMs containing both PA-HGO-4h studied by SEM. Characterization of MOF-filled PA dense membranes. The top-view images (**Figure 2**) are very similar for all membranes (including pure PA A), where no pinholes or defects are observed within the resolution of the SEM.

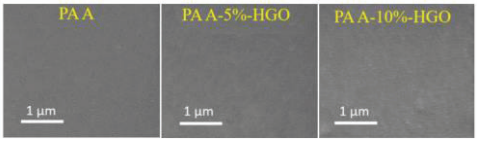

Figure 2. Top-view SEM images of PA A membranes (a) and PA A-5%-HGO (b) and PA A-10%-HGO (c).

3.2. Gas transport properties

3.2.1. Effect of chemical structures on gas transport properties

The mean gas permeability coefficients and ideal permselectivity values for four different gases (CO_2, O_2, N_2 and CH_4) of the MMMs are tabulated in the **Table 2.** The gas permeability of four different gases through these MMMs membranes follow the order of P (CO_2) > P (O_2) > P (N_2) > P (CH_4). The contribution of the HGO to the membrane separation performance of the resulting MMMs was evaluated first using

dense membranes. HGO in PA membranes at 3 bar and 35 ºC was measured. Moreover, increase in selectivity with increasing filler loading for the 8HGO-filled PA-membranes at 10 wt% loading. Just like for the polymer, the selectivities in the HGO can be ascribed to the differences in the electrostatic interaction of different gas molecules with the membrane constituents: CO_2 has a strong quadrupole moment, while CH_4 has none, thus showing increased interactions, hence sorption, in a polar environment like the HGO framework.

Table 2 Gas permeability coefficients (P) measured at 35 °C (3.5 bar) and permselectivities (α) values of the MMMs and their comparison with other reported polymers.

MMMs	P(CO_2)	P(O_2)	P(N_2)	P(CH_4)	α(CO_2/CH_4)	α(O_2/N_2)	Ref.
PA A	9.00	2.40	0.45	0.35	26.00	5.30	[8]
PA A-5%-HGO	15.00	4.30	0.85	0.70	21.50	5.00	This study
PA A-10%-HGO	40.0	11.0	1.60	1.20	33.50	6.90	This study

[a]Gas permeability coefficient (P) values taken from ref. [1]. P = gas permeability coefficient in barrer. 1 barrer =10^{-10} cm^3 (STP) cm cm^{-2} s^{-1} cm^{-1} Hg^{-1}.

3.2.2. Comparison of gas permeabilities of MMMs with structurally related polymer membranes

The gas permeability and permselectivity values of these MMMs PAs (PA A 5-10%-HGO) was compared with other commercially available polymers (e.g., Matrimid®, Extem® and Ultem®) and some previously reported polymer (3g, 3h and P3)[1,2]. A better comparison of the CO_2/CH_4 permselectivity vs. CO_2 gas permeability (**Figure 3**) have been obtained in terms of the Robeson plots[2]. The good permselectivity values of PA A-5%-HGO for CO_2/CH_4 gas pairs were credited to their higher diffusivity selectivity values. The present PAs showed good improvements in gas-separation performance as proved by their trade off points close to the Robeson's upper bound.

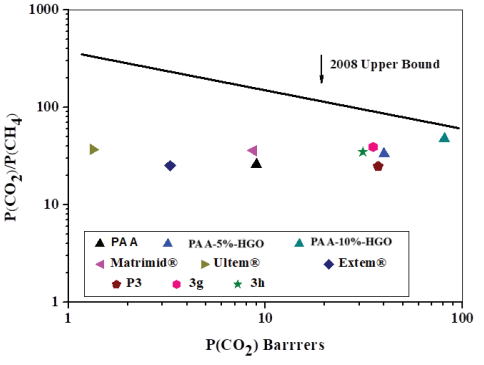

Figure 3. Robeson plot of CO_2/CH_4 selectivity vs. CO_2 and some other reported polymers[1].

4. Conclusions

In this study, a strategy to improve the long-term performance of PA by the addition of holey GO-based nanofillers have been reported, and chemistry and the porosity of the nanofiller play an important role in the performance of the MMMs. The priming protocol to prepare the MMMs resulted in a good distribution of fillers in the polymer matrix. The gas transport studies showed that the incorporation of the HGO improved both the gas permeability and permselectivity of these polymer membranes. The increasing permeances with increasing HGO-loadings were attributed to the structural properties of the HGO.

4. References

1. Bisoi S, Bandyopadhyay P, Bera D, Banerjee S. Effect of bulky groups on gas transport properties of semifluorinated poly (ether amide) s containing pyridine moiety. European Polymer Journal. 2015 May 1;66:419-28.

2. Luque-Alled JM, Tamaddondar M, Foster AB, Budd PM, Gorgojo P. PIM-1/Holey graphene oxide mixed matrix membranes for gas separation: unveiling the role of holes. ACS applied materials & interfaces. 2021 Nov 10;13(46):55517-33.

MICROBIAL LIPID- A NEW SOUSE OF BIOSURFACTANT

Dr. Soma Das

Center for Distance and Online Education
Vidyasagar University
Email: somadasddevu@gmail.com

Abstract

Microbial lipids are collected from microbes, especially from oleaginous fungi and yeasts. These microbial lipids are well known as biosurfactant Biosurfactants are surface-active compounds that have sparked interest in recent years because of their environmental advantages over conventional surfactants. The aim of this study is to investigate the production of biosurfactants from fungi isolated from soil. Fungi colonies were isolated from soil samples and screened for biosurfactant production in submerged fermentation. In addition, the influences of bioprocess factors (carbon source, nitrogen source, pH, and fermentation time) have investigated. Finally, the biosurfactant produced was semipurified and submitted to stability test as emulsifier.

Keywords: Microbial lipid, Biosurfactants, Fungi, Fermentation, Emulsifier

Introduction

Biosurfactants are produced by microbes, a surface active biomolecules. Its are unique ampiphilic molecule and distinguished from synthetic surfactants only on the basis of their origin. Biosurfactants include wide rance of surfactants and emulsifier such as glycolipids, glycerophospholipids, glycosphingolipids bile acid, protine etc (1)

A number of bio-surfactants are obtained economically from micro-organism such as *Penicilium spiculisporum* (2), *Pseudomonous sp* (3), *Bacillus subtilis* (4), *Acinetobactor calcoaceticus* (5), *Corynebacterium hydrocarboclastus* (6) *and Pseudomonus aeruginosa* (7).

Initially glycolipid surfactants were first developed as bio-surfactant (8), Growth of Arthrobacter sp. DSM 2567 in a culture medium containing glucose and mannose led to the formation of the corresponding glycolipids esterified at the C-6 position with and alpha-branched beta-hydroxy fatty acid. Cellobiose corynomycoplates were low in studies with growing culture. However after separation of the cell growth production phase, the yields rose when resting cells in a phosphate buffer were used. The energy gained by degradation of the carbohydrates was high enough to permit the synthesis of glycolipids over several days. The glycolipids were emulsified with

synthetic deposit water. Strongest reduction in surface tension and interfacial tension down to around 35 and 1 mN/m were obtained with the more hydrophilic substances high saline solution suggesting the use of glycolipids in tertiary oil recovery (9).

Micobacterium kansaii an important entiologocal agent of chromic pulmonary infections was found to contain a novel kind of antigenic mannose containing phenolic glycolipid (10).

Phodococcus erythropolis DSM 43216 produced a trehalose – 2,2; 3,4-tetra ester when grown on n-alkanes. Product from this bacteria showed surface activities (11).

A strain Pseudomonus putida 21BN (12) produced a surfactant which substantially changes the surface tension of the culture medium when grown on hexadecane.

Pseudomonas aeruginosa LB1, isolated from petroleum-contaminated soil (13) was incubated in a mineral salt medium [14] with the composition (g/L): 4.0 $NaNO_3$, 1.0 K_2HPO_4, 0.5 KH_2PO_4, 0.5 $MgSO_4$, 7 H_2O, 0.1 KCl, 0.01 $FeSO_4$, 7 H_2O, 0.01 $CaCl_2$, 0.01 Yeast extract and 0.05 ml/L of the solution of the trace element (B, Cu, Mn, Mo and Zn) at 30°C for 86h. Rhamnolipids were produced which act as surfactant by decreasing the surface tension from 72mN/m to 24mN/m and from the biological and physicochemical properties, it could be used as antimicrobial and emulsifier agent in the agrochemical and food industry.

Certain microorganisms, such as *Bacillus subtilis, Pseudomonas aeruginosa, Torulopsis bombicola* have been reported to utilize crude oil & hydrocarbons as sole carbon sources & can be used for oil spill clean-ups [15]. These strains are used to produce biosurfactant.
There is a detailed study on the wide range of applications of biosurfactants in medicine by Mukherjee et al. [16].

A good example is the biosurfactant produced by *marine B. circulans* that had a potent antimicrobial activity against Gram positive and Gram negative pathogens and Semi pathogenic microbial strains including MDR strain. [17]

Trehalolipids contain trehalose disaccharides associated with a fatty acid (mycolic acid), have high structural diversity, and are mainly produced by species of the genera *Rhodococcus, Nocardia, Mycobacterium and Corynebacterium* [18].

Replacing synthetic surfactants with biosurfactants would reduce lifetime CO2 emissions by 8%, leading to the avoidance of an estimated 1.5 million tons of CO2 released into the atmosphere [19].

Materials & Method

The enzyme Rhizomucor miehei (lipozyme, RMIM) and lipozyme TL IM used as catalyst were gift of NOVOZYME South Asia Pvt. Ltd, Bangalore, India.

Dextrose was supplied by s.d. Fine CHEM Pvt. Ltd., Kolkata.

Yeast was purchased from SRL Chemicals Ltd., Ammonium nitrate was collected from s.d. Fine CHEM Pvt. Ltd., Kolkata, Potato was purchased from local market.

Production of Bio-surfactant from microorganism

Organism: Rhizopus nigrican (SB12), Fusarium (S1)

Isolation of Fungi from Soil by Serial Dilution

10 gm of the soil diluted with 90 ml of sterile distilled water is further diluted in the order of 10^2, 10^3 and 10^4 with sterile distilled water. 1 ml of each of these diluted samples is them added to 20 ml of potato-dextrose-yeast-agar medium in petri-dishes. The potato-dextrose-yeast-agar medium contains extract of sliced 100 gm potato, 5.0 g yeast extract 20.0 gm dextrose and 20.0 gm agar per litter of the medium, pH of the medium being kept at 6. The fermentation medium contains no organic and inorganic salt. Along with the medium oxy-tetra cycline hydrochloride in the concentration of 125/150 mg is added to inhibit the growth of bacteria. The petri dishes were incubated for 24 hrs at 30°C.

The colonies obtained on petridishes are then isolated by repeated inoculation in potato-dextrose-yeast-agar slants till growth of a single kind is found. The fungi obtained are then identified under microscope.

Cultivation of Fungi

The pure fungi are then cultivated in 100 ml of liquid medium mentioned above varying dextrose concentration and incubation with addition of different minerals at 30°C.

Extraction of Fungi and Fungal Lipids

The fungal biomass is harvested by filtration, dried at 50°C under vacuum for 5 hours, weighed and subjected to solvent extraction in a Soxhlet apparatus with 2:1, 1:1 and 1:2 chloroform and methanol in dark. Methanol is collected and the chloroform being removed under ordinary heating and vacuum. The total lipid content is determined by weighing and surface activities of the microbial lipids collected from different micro-organism are determined.

Measurement of Surface Property and Emulsification Properties

The Interfacial tension of chloroform as well as chloroform solution of of different biosurfactant against water are determined by well-known drop weight method based on the equation –

$$\gamma_{I/II} = (\rho_I - \rho_{II})\, v g / 2\pi r f \ldots\ldots\ldots\ldots\ldots\ldots\ldots\ldots \quad [20]$$

Where γ = interfacial tension at the liquid I and II interface, ν =volume of the drop of the liquid, g =gravitational acceleration, r= radius of the capillary (< 1 mm), f= correction factor. The measurement was done for 10 drops in all cases. All the measurements were done at 27^0C.

Result & Discussion

Three microbial strains – *Rhizopus Nigrican (SB12), Fusarium (F1)* are used for the production of biosurfactant. The microbe are grown in potato-dextrose-yeast medium. The nitrogen source is an important key to the regulation of biosurfactant synthesis. Yeast can serve as a nitrogen source. The lipid content, moisture content and biomass of microbial growth with variation of dextrose concentration in the culture medium are presented in Table-1.

The lipid content in Rhizopus Nigrican (SB12) and A1increases with the concentration of dextrose but the accumulation of lipid in S1increases between certain concentration of dexrosein the medium and the lipid content decreases at high concentration. The analytical information at optimum condition is given in Table-2.

It is evident from the TLC picture that these three lipid contains some phospholipid and triglyceride (TG). The phospholipid is the major component of the microbial membrane.

There is a salt effect on the lipid content of the microbial growth. The result of salt effect study is shown in Table-3.In presence of 0.3% ammonium nitrate in culture medium the lipid content in Rhizopus nigrican- SB12 changes from 13.0 to 14.3%, for Fusarium-S112.4 to 14.3% and for A1 from 12.2 to 15.0%.

The values of interfacial tension at chloroform-water interface and CMC value of three microbial lipids are given in Table-4. The interfacial tension of 0.1% solution of these microbial lipid shows significant lowering of interfacial tension which is comparable to 0.1% chloroform solution of phospholipid.
From the all above discussion it is established that the microbial lipids collected from *Rhizopus Nigrican (SB12)*, and *Fusarium (S1)* show distinct surface active properties which lead to treat them as biosurfactant.Microbial lipids revealing distinctly surface active properties like the lowering of surface tension and ability to form stable emulsion and known as bio-surfactants could be isolated from some microbial strains. Three microbial strains are used for the production of microbial lipids when grow in appropriate medium.

Table-1: Analysis of Moisture, Bio-mass and Lipid Content of Microbial Growth at Different Dextrose Concentration of Culture Medium

Sample	Dextrose concentration Gm/L	Analysis of Microbial Growth		
		Moisture content (%)	Bio-mass content (Gm/L)	Lipid content (on dry basis) (%)
SB 12	20	85.3	3.5	3.7
	40	87.3	5.1	7.6
	200	76.8	8.3	9.6
	20	87.3	5.7	5.6
S 1	40	81.3	8.4	7.1
	200	65.3	14.8	4.45

Table-2: Analysis of Microbial Growth (Containing 200 gm/L Dextrose in Culture Medium after 4 Days)

Sample	Moisture Content (%)	Weight of Dry Bio-mass (in 200 ml)	Bio-mass Gm/L	Lipid Content (%)
SB 12	76.8	1.65 gm	8.25	9.6
S 1	65.3	2.96 gm	14.8	5.4

Table-3: Effect of Salt on the Lipid Content (Lipids are Collected from the Microbes after 4 Days)

Medium Condition	SB 12	A 1	S 1
Medium without Salt	13.0 (%)	12.2 (%)	12.4 (%)
Medium with Salt (0.3% Ammonium Nitrate)	14.3 (%)	15.0 (%)	14.3 (%)

Table-4: Studies of Surface Properties of Microbial Lipids

Sample	Interfacial Tension (mN/m) (0.1%Chloroform Solution)	Critical Micelle Concentration (gm/lit)
SB 12	17.3	2.5
S 1	18.4	1.0

Conclusion

The salient features emerging from the following research works are highlighted as follows:

- The microbial lipids collected form Rhizopus nigrican (SB 12), and Fusarium (S 1) display surface active properties.
- The presence of a salt like ammonium nitrate in the medium plays an important role favouring the synthesis of lipid in microorganism.

Therefore bio surfactant produced by fungi becomes a versatile and sustainable alternative that should be encouraged, in view of society's demands for ecologically safe products obtained through green technologies

Reference

1. S. Kudo, Proceedings of the World Conference on Biotechnology for the Fats and oils Industry, *American Oil Chemists' Society*, Ed., Thomas H. Applewhite, p. 195 (1998)

2. Tabuchi T., et al., Accumulation of the open-ring acid of spiculisporic acid by *Penicillium spiculisporum* in shake culture, J. Ferment. Technol., 55:37 (1977)
3. Wilkinson S.G., Composition and structure of the ornithin-containing lipid from Pseudomonas Rubescens, Biochem. Biophys. Acta., 270:1 (1972)
4. Arima, K., Atsushi Kakinuma and Gakuro Tamura, Surfactine, A cryatalline, peptidolipid surfactant produced by Bacillus subtilis, *Biochem. Biophys. Res. Com.,* 318:488 (1968)
5. Rosenberg, E., A. Zuckerberg, C. Rubinovitz and D. L. Gutnick, Emulsifier of arthobacter RAG-1: isolation and emulsifying properties*, Appl. Env. Microbiol.,* 37:402 (1979)
6. Zajic J. E., et al., Emulsifying and surface active agents from Corynebactirium hydrocarboclustus, *Biotech. Bioeng*. 19: 1285 (1977)
7. Jarvis F. G. And M. J. Johnson, *J. Am. Chem. Soc.*, 24:4124 (1949)
8. Inoue S., Proceedings of the World Conference on Biotechnology for the Fats and Oils Industry, *American Oil Chemists' Society*, Ed., Thomas H. Applewhite, P. 206 (1988)
9. Li. Z. Y., S. Lang, F. Wagner, L. Witte and V. Wray, Formation and identification of interfacial-active glycolipids from resting microbial cells, *Appl. Environ Microbiol*. 48: 610 (1984)
10. Reviere M., J. J. Fournie and G. Puzo, A noval mannose containing phenolic glycolipid from *Mycobacterium* kansasii, *J. Biol. Chem*. 262: 114879 (1987)
11. Kim, J. S., M. Powalla, S. long, F. Wagner, H. Luendorfahd and V. Wray, Microbial glycolipid production under nitrogen limitation and resting cell condition, *J. Biotechnol*. 13: 257 (1990)
12. Borjana, K. Tuleva, George R. Ivanov and Nelly E. Ghrostova, Z., Biosurfactant Production by a new *Pseudomonas putida* strain, *Naturforsch*. 57C: 356-360, (2004)
13. Benincase, M., A. Abalos, I. Olivera and A. Aanresa, Chemical structure, surface properties and biological activity of the biosurfactant produced by Pseudomonas aeruginosa LB1 from soapstock, *Autonie Van Leenwenhoek*, 85: 1-8 (2004)
14. Suparna Basu, Ph. D. (Tech) thesis of, Calcutta University, *'Studies on Lipase Catalysed Process Technologies in Making Certain Fatty Acid Derivatives for Better Utilization'* pp – 105, (1998)
15. Das K, Mukherjee AK - Crude petroleum-oil biodegradation efficiency of Bacillus subtilis and Pseudomonas aeruginosa strains isolated from petroleum oil contaminated soil from North-East India. Bioresource Technol -98: 1339- 1345. (2007)
16. Mukherjee S, Das P, Sen R- Towards commercial production of microbial surfactants. Trends Biotechnol 24: 509-515. (2006)
17. Gharaei-Fathabad E - Biosurfactants in pharmaceutical industry: A Mini – Review. American Journal of Drug Discovering and Development 1: 58-69. (2011)
18. G. Rawat, A. Dhasmana, V. Kumar -Biosurfactants: the next generation biomolecules for diverse applications Environ. Sustain., 3, pp. 353-369, (2020) 10.1007/s42398-020-00128-8

19. I.M. Banat, Q. Carboué, G. Saucedo-Castañeda, J. de Jesús Cázares-Marinero Biosurfactants: the green generation of speciality chemicals and potential production using Solid-State fermentation (SSF) technology Bioresour. Technol., 320 (2021), Article 124222, 10.1016/j.biortech.2020.124222
20. Harkins, D. and F. E. Brown – Determination of surface tension(free surface energy) and the weight of falling drops. The surface tension of water and benzene by the capillary height method – Journal of American Chemical Society XLI, P: 499-524, (1919)

BIOSYNTHESIS OF AG NANO PARTICLES (AGNPS) AND ITS APPLICATION

Madhumita Hazra
Department of Chemistry, PRMS Mahabidyalaya, Jamboni, Bankura- 722150, India
Email: hazra.madhumita.hazra@gmail.com

Abstract

Nanoparticles are an important part of nanotechnology. Several approaches which comprise physical and chemical methods have been used for the synthesis of the nanoparticles. The nanoparticles have many sizes, shapes, and compositions, so maintaining the particular properties is a very vital task in the area of nanoscience. The clinical application is limited if the nanoparticles are synthesized by the use of non-polar solvents and toxic chemical reagents. For this reason, the synthesis of nanoparticles using non-toxic, eco-friendly, and biocompatible methods have been developed. Among the various nanoparticles silver nanoparticles (AgNPs) is one of the most important nanoparticles which have unique properties. Synthesis of AgNPs by using plant extract, bacterial strains, fungus etc. are described here with various applications.

Keywords: Nano particles, Bio-synthesis, Applications.

1. Introduction

Nanoparticles have dimensions between approximately 1-100 nanometre. There are two major techniques for the synthesis of nanoparticles, “top down” and “bottom up” approaches. In the top-down method the tools are used to cut and shape the materials to give the desired shape to the materials. But the most effective and acceptable approach is the bottom-up approach for the synthesis of nanoparticles. In the bottom-up approach, the smaller building blocks such as molecules or atoms self-assembly together to form a nanoparticle. By this method it is possible to maintain the shape and size of the synthesized nanoparticles. Silver nanoparticles (AgNPs) are prepared from different perspectives, some researchers have used chemical methods for the preparation of silver nanoparticles (AgNPs) [1]. They have application in catalysis, electronics, drugs and they control the development of microorganisms in the biological systems which made them eco-friendly [2]. The biosynthesis of AgNPs involves plant extracts, bacteria, fungi, yeast etc. [3]. In recent years, the parts of plants such as leaves, fruits, flowers, besides this the enzymes are used for the preparation of silver nanoparticles (AgNPs) [4]. Now a days there is a problem of in increasing the bacterial and viral strains due to mutations, changing in environmental conditions, for this problem the scientists are searching for drug for the treatment of

these microbial and viral infections. There are many metal nanoparticles which prevent the growth and infection of bacteria. Silver nanoparticles (AgNPs) are one of those important metal nanoparticles which occupy an important place for preventing the growth of the microbial. It is reported that the small sized silver nanoparticles (AgNPs) are the excellent inhibitor of growth of certain bacteria. Several reviews have been published on the silver nanoparticles (AgNPs) but there are few reviews on their green synthesis [5]. In this chapter, the green synthesis of silver nanoparticles (AgNPs) from the green sources and their potential applications is discussed.

2. Synthesis and characterization of AgNPs

Synthesis of silver nanoparticles (AgNPs) is an important aspect of nanotechnology. The size, shape, structure, physical, chemical and biological properties of nanoparticles depend on the synthetic method. Several synthetic methods have been reported by the researchers. Mainly, the three most important approaches have been given.

1. Chemical methods
a. Pyrolysis
b. Electrochemical method
c. Irradiation-assisted chemical method
d. Chemical reduction method
2. Physical methods
3. Biological methods
a. Using plant extract
b. Using Bacteria
c. Using Fungi
d. Using Algae

The chemical reduction method is the most common and widely used method which involves the reduction of Ag^+ species to Ag° using reducing agents like $NaBH_4$, $LiAlH_4$, etc. Physical methods usually involve high-energy consumption during synthesis. In biological methods, AgNPs have been synthesized by using fungi, plants, bacteria and algal extracts and do not employ any toxic reducing agents.

2.1 Synthesis of AgNPs from plant extracts:

The silver nanoparticles have wide applications in the field of medicine, biotechnology, microbiology, optics and material science which increased their demand in chemical industries. For the synthesis of silver nanoparticles various reducing agents are used such as hydrazine, Tollen's reagent, H_2 gas, ethanol, and aliphatic amines [6]. The reducing agents can be used to control the particle size of the nanoparticles. Plants contain fat, carbohydrates, nucleic acids, proteins, which act as a reducing agent for the synthesis of nanoparticles from metal salts. This process is free from producing any toxic by-product. Plant parts such as roots, steam, flowers, leaves and seed have been used for the synthesis of silver nanoparticles [7]. The plant mediated synthesis of Ag nanoparticles is given below-

• Plant name- Aloe vera, plant part- Leaf gel, the synthesized nanoparticles have size range between 5-50 nm and octahedron shape. Flavanones and terpenoids are responsible for the reduction of silver nitrate.

• Plant name – Mangifera indica, plant part- Seed, the synthesized nanoparticles have size range 14 nm and spherical and hexagonal shape. Phenolic compounds, gallotannins and tannin are responsible for reduction of silver nitrate.

• Plant name- Carambola, plant part- Fruit, the synthesized nanoparticles have size range between 16, 13, 12 nm at pH 4, 7, 10 respectively and spherical shape. Polysaccharides, polyols and ascorbic acid are responsible for the reduction of silver nitrate.

• Plant name- Piper nigrum, plant part- seeds, the synthesized nanoparticles have size range between 10–60 nm; rod shaped, Polysaccharides, amino acids, alkaloids, proteins and vitamin are responsible for the reduction of silver nitrate.

• Plant name-Piper betle, plant part- Leaf, the synthesized nanoparticles have size range between 48–83 nm; spherical, Allylic benzenes, phenolic, amino acids, proteins, alcoholic compounds, terpenes and terpenes are responsible for the reduction of silver nitrate.

• Plant name- Trigonella foenum-graecum, plant part- seeds, the synthesized nanoparticles have size range between 20–50 nm; spherical, Saponins and alkaloids are responsible for the reduction of silver nitrate.

• Plant name- Calotropis procera, plant part- flower, the synthesized nanoparticles have size range between 35 nm; face centered cubic; Tannins, triterpenes, favonoids, steroids, alkaloids are responsible for the reduction of silver nitrate.

• Plant name- Picrasma quassioides, plant part- Bark, the synthesized nanoparticles have size range between 17.5–66.5 nm; spherical.

• Plant name- Sterculia acuminata, plant part- Fruit, the synthesized nanoparticles have size range between 10 nm; spherical, Ascorbic acid, gallic acid, phenolic compounds, pyrogallol, methyl gallate and polyphenolic are responsible for the reduction of silver nitrate.

• Plant name- Terminalia cuneata, plant part- Bark, the synthesized nanoparticles have size range between 25–50 nm; spherical, Tannins, saponins, triterpenoids, favonoids, gallic acid, ellagic acid and phytosterols are responsible for the reduction of silver nitrate.

• Plant name- Cirsium japonicum, plant part- plant, the synthesized nanoparticles have size range between 4–8 nm; spherical, Saponins, proteins and favonoids are responsible for the reduction of silver nitrate.

• Plant name- Isatis tinctoria, plant part- plant, the synthesized nanoparticles have size range between 10–15 nm; spherical, Saponins and favonoids are responsible for the reduction of silver nitrate.

• Plant name- Aegle marmelos, plant part- Fruit, the synthesized nanoparticles have size range between 22.5 nm; spherical, hexagonal, roughly circular, Phytosterols, favonoids, alkaloids, terpenoids and amino acids are responsible for the reduction of silver nitrate.

2.2 AgNPs from bacterial strains

Recently the biosynthesis of AgNPs from bacteria has been developed. Some bacterial strains have been used for biosynthesis of AgNPs.

• Bacteria name- Pseudomonas aeruginosa BS-161R, the synthesized nanoparticles have Size and shape- 15.1 ± 5.8 nm; spherical Bio-surfactants- Rhamnolipids.

• Bacteria name- Bacillus cereus NK1, Size and shape- 50-80 nm; spherical Bio-surfactants- URAK (a fbrinolytic enzyme).

• Bacteria name- Gluconacetobacter xylinum, Size and shape- 5–40 nm Bio-surfactants- Cellulose.

• Bacteria name- Streptomyces coelicolor, Size and shape - 28–50 nm; irregular Bio-surfactants- Actinorhodin pigment.

• Bacteria name- Bacillus subtilis MSBN 17, Size and shape - 60; spherical Bio-surfactants- Biofocculant.

• Bacteria name- Bacillus athrophaeus Size and shape - 5–30 nm; polydispersed Bio-surfactants- Spores.

• Bacteria name- Nostoc commune Size and shape - 15–54 nm; spherical Bio-surfactants- Extracellular polysaccharide/matrix.

• Bacteria name- Gordonia amicalis HS-11 Size and shape - 5–25 nm; spherical Bio-surfactants- Glycolipid.

• Bacteria name- Acinetobacter calcoaceticus Size and shape- 8–12 nm; spherical Location- Extracellular.

• Bacteria name- A. haemolyticus MMC8 Size and shape- 4–40 nm Location- Extracellular.

• Bacteria name- Aeromonas sp. SH10 Size and shape- 6.4 nm Location- Extracellular and intracellular.

• Bacteria name- Bordetella sp., Size and shape- 63–90 nm Location- Extracellular.

2.3 Synthesis of Ag nanoparticles from fungi:

The biosynthesis of silver nanoparticles (AgNPs) from both pathogenic and non-pathogenic fungi has been developed. The silver ions are reduced in presence of fungi to produce stable AgNPs in water.

• Fungus- *Aspergillu flavus*, Size and shape of AgNPs- 8.92 nm; spherical Synthesis location- Extracellular.

• Fungus- *A. terreus*, Size and shape of AgNPs- 1-20 nm; spherical Synthesis location- Extracellular.

• Fungus- *Coriolus versicolor*, Size and shape of AgNPs- 25-75 nm; spherical, Synthesis location- Extracellular and intracellular.

• Fungus- *Humicola sp.*, Size and shape of AgNPs- 5-25 nm; spherical, Synthesis location- Extracellular.

• Fungus- *Macrophomina phaseolina*, Size and shape of AgNPs- 5-40 nm; spherical, Synthesis location- Cell-free filtrate.

3. Applications of AgNPs:

AgNPs has distinctive physical, chemical and electrical properties, as they have numerous applications in different fields like medicines, electronics, water treatment, chemical and food industry, etc. Due to these extensive applications of AgNPs, their synthesis has gained a lot of attention from researchers worldwide.

Medical Applications:

(a) Catheters: Catheters used in the hospital, have a high penchant for contamination, that can lead to undesirable complications. Polyurethane catheters have been made efficient by the Ag-coating which enhance the activity. (b) Wound dressing: Ag injury dressings have been used to clinically treat different injuries, with no unfriendly impacts as compare to standard Ag Sulfadiazine and gauze dressing. Ag nanoparticles used in wound dressing gives better result. (c) Cardiovascular impact: First cardiovascular device coated with Ag element heart valve to diminish the occurrence of endocarditic. (d) Dentistry: Silver nanoparticles a major Nanoparticles have been used in dental instruments and bandages. Ag Nanoparticles increase the shear bond strength of an orthodontic adhesive while expanding its resistance to bacteria. They also enhance the antifungal activity. (e) Anti-cancer agents: Nowadays, AgNPs are widely used as a therapeutic agent, in the diagnosis and treatment of cancer. This is because the toxicity of silver nanoparticles towards cancerous cells is more as compared to the bulk materials. (f) Drug delivery system: AgNPs are also being used for targeted drug delivery now a day. Its effectiveness in delivering the anti-cancer drugs to the tumour tissue has already been observed.

Antimicrobial agent:

The silver nanoparticles show antibacterial activity. They exhibit inhibitory activity against gram positive and gram-negative bacteria. They have also antimicrobial and antiviral activity and anti fungal activity.

Industrial Applications:

Catalysis: The silver nanoparticles are used as catalyst in many reactions as for example CO oxidation, benzene oxidation to prostaglandin, phenol and the reduction of the pnitrophenol to p-aminophenol. Silver nanoparticles are immobilizer on siloca spheres for the catalysis of the reaction of the dyes by sodium borohydride ($NaBH_4$].

Agriculture engineering:

Nanosized silver nanoparticles are obtained from harvests and trees. These can be used in food packaging and other material packaging. Nanofertilizers that are very useful, have good capacity to synchronize slow release of nutrient with their ability of plant uptake. This can be accomplished by averting nutrient from interacting with microorganisms, soils and water.

Nano-biosensors:

Nanoparticles are very exceptional characters for various biosensors as they can be detected by various different methods. By utilizing SPR, the silver nanoparticles can attain very much high sensitivity and measurements. Ag Nanoparticles have improved a variety of Nanoparticles in their function ability.

Sensors:

Environmental monitoring is the course of accessing the environmental situation to check the attention of pollutants in the nearby. Several toxic metals can be present in the environment similar to mercury, cadmium, lead, copper, nickel, chromium, etc. Due to current advancements in nanotechnology, it has been found that silver nanoparticles can be capably used in optical sensing for the finding of heavy and toxic metals.

4. Conclusion:

In this review covers the several approaches of synthesis of silver nanoparticles and its scope of applications. The synthesis of AgNPs from the green sources like the plant extracts, bacteria, fungi and algae. The size and shape of the AgNPs are also known. This AgNPs are used as health care materials, bio-sensors, bio-technology, agriculture, catalysis, electronics and antimicrobial agent. They are used to prevent both the gram positive and gram-negative pathogens. Silver nanoparticles are active against many drugs resistant bacteria. They are used to prepare easily available medicine for the treatment of many infections. AgNPs are often used in the drug delivery systems.

Reference:

1. Rafique S, Bashir S, Akram R, Jawaid S, Bashir M, Aftab A, Attique A, Awan SU. In vitro anticancer activity and comparative green synthesis of ZnO/Ag nanoparticles by moringa oleifera, mentha piperita, and citrus lemon. Ceramics International. 2023 Feb 15;49(4):5613-20.

2. Wasilewska A, Klekotka U, Zambrzycka M, Zambrowski G, Święcicka I, Kalska-Szostko B. Physico-chemical properties and antimicrobial activity of silver nanoparticles fabricated by green synthesis. Food Chemistry. 2023 Jan 30;400:133960.

3. Essghaier B, Hannachi H, Nouir R, Mottola F, Rocco L. Green Synthesis and Characterization of Novel Silver Nanoparticles Using Achillea maritima subsp. maritima Aqueous Extract: Antioxidant and Antidiabetic Potential and Effect on Virulence Mechanisms of Bacterial and Fungal Pathogens. Nanomaterials. 2023 Jun 28;13(13):1964.

4. Siddiqi KS, Husen A, Rao RA. A review on biosynthesis of silver nanoparticles and their biocidal properties. Journal of nanobiotechnology. 2018 Dec;16(1):1-28.

5. Nguyen NP, Dang NT, Doan L, Nguyen TT. Synthesis of Silver Nanoparticles: From Conventional to 'Modern'Methods—A Review. Processes. 2023 Sep 2;11(9):2617.

6. Bhui DK, Bar H, Sarkar P, Sahoo GP, De SP, Misra A. Synthesis and UV–vis spectroscopic study of silver nanoparticles in aqueous SDS solution. Journal of Molecular Liquids. 2009 Mar 15;145(1):33-7.

7. Beyene HD, Werkneh AA, Bezabh HK, Ambaye TG. Synthesis paradigm and applications of silver nanoparticles (AgNPs), a review. Sustainable materials and technologies. 2017 Sep 1;13:18-23.

ISOLATION AND FUNCTIONALIZATION OF DIAMONDOIDS: ROLE OF GREEN CHEMISTRY

Shiladitya Banerjee

Department of Chemistry, Midnapore College (Autonomous), West Midnapore, West Bengal, India, Pin-721101
E-mail: shiladitya.banerjee@midnaporecollege.ac.in

Abstract

Isolation of diamondoids from petroleum and their synthesis and functionalization have been an active area of research since the past few decades, owing to the interesting set of physical, chemical and optical properties possessed by this class of saturated hydrocarbons, whose structure resemble the diamond lattice. However, traditional methods of isolation and chemical reactions involve the use of toxic and environment-threatening reagents and solvents, which are of high concern. This review provides insight into some of the very recent developments in the application of green chemistry in extraction of diamondoids and preparation of their derivatives

Keywords: Diamondoids, green chemistry, non-ionic surfactants.

1. Introduction

Diamondoids categorize a class of saturated hydrocarbons resembling the diamond lattice, which possess a set of attractive chemical and physical properties, such as thermal stability, remarkable hardness, resistance to chemical and microbial action, high refractive index and melting point and strong photoluminescence[1]. The pristine diamondoids (adamantane and higher homologues) were first isolated from petroleum; since 1933[2].

Due to their properties, they have a wide variety of industrial and chemical applications. They are used in ultraviolet and blue organic LEDs, as recyclable, porous catalysts, rendering additional stability to drugs, providing stability and enhancing the refractive indices and lowering the dielectric constants of metal nanocomposites[3,4,5]. Large scale, wide-variety applications demand a steady supply and coupled with the fact that it is considerably practical to introduce functional groups into diamondoids and modify their electronic and optical properties, isolation and synthesis of diamondoids have always been an active field of research for chemists[6].

Standard chemical reactions, such as halogenation (catalyzed by Lewis acids), nitration, amination, alkylation, thiourea mediated thiolation and metal mediated C-C

coupling of halogenated diamondoids, have been used for preparing substituted diamondoids[7, 8].

Naturally occurring diamondoids (and some of their alkylated derivatives) are found in petroleum; believed to be formed by rearrangement reactions of hydrocarbons in prevailing acidic conditions[9,10]. Traditional isolation methods include solvent extraction process by using organic solvents, such as dichloromethane, hexane and chloroform (which are toxic and harmful for the ozone layer), under harsh physical conditions, generating toxic organic wastes, with disposability issues[11]. It is in this context that green-chemistry, which refers to the use of environment friendly chemicals and methods, comes into play for isolation and extraction of diamondoids. Non-ionic surfactants, owing to their non volatility and environment friendliness are effective green solvents for extraction of polar, as well as, non-polar organic substances from solid matrices/samples.

2. Green Chemistry and Diamondoids

Schmidt and co-workers have used Microwave assisted non-ionic surfactant extraction (abbreviated as MANSE) for extracting diamondoids from petroleum source rock[12]. The samples were ground and passed through porous sieves prior to extraction. Hazard-less solvents, such as polyoxyethylene (23)dodecyl ether and polyoxyethylene (10)dodecyl ether were used to extract adamantane and diamantane and at the high extraction temperature (around 110^0C, increasing chain length of the ether provided more efficient extraction.

The extractions were designed by pre-optimization of extraction temperature, extraction time and concentration of the non-ionic surfactant solution by using a linear-fit model for yields of diamondoids. The extraction temperature was found to be the most important factor controlling the efficiency of the extraction; which is expected, since a lower temperature leads to lower rate of extraction. A temperature of 80^0C and an extraction time of 10 minutes proved to be the most optimum conditions for extracting adamantane, diamantane and their alkylated derivatives, such as 2-Ethyladamantane. The extracted diamondoids were analyzed using gas-chromatography – mass spectrometric analysis.

In another quite-recent work[13], scientists have synthesized diamondoid ethers by the green chemical procedure of high temperature ball milling, from Iodo-diamondoid and the corresponding alcohol. This mechanochemical method involved the grinding of nanostructures (using stainless steel balls, in Teflon jars kept in aluminum containers) into fine powders and the use of a high temperature of 200 degrees, providing the necessary activation energy for ether formation. The method involved an environment-friendly and hazard-less inorganic base (K_2CO_3) and provided higher yields and needed shorter reaction times (3 hours), compared to methods involving the use of traditional solvents such as dichloromethane, for 4-24 hours[13,14].

1,1'Diadamanthyl ether was obtained at 65% yield from 1-Adamantanol and 1-Iodoadamantane, using the above-mentioned procedure, while a 42% yield was obtained for 1-Adamantyl-4-diamantyl ether. Many other ethers, such as 1-Diamantyl-4-diamantyl ether, 4,4'-Didiamantyl ether and others were obtained from various

positional isomers of adamantane and diamantane. The yields of the products varied from around 42% to 70%.

3. Conclusion

Green chemical methods provide promising alternatives for extraction of diamondoids from natural sources, such as petroleum and preparation of their derivatives, without the use of toxic and hazardous chemicals, which are harmful for the environment and pose disposal problems. Although the isolation of diamondoids date to the 1930s and 40s, the large-scale synthesis and derivatization using traditional chemical methods have gained considerable popularity and interest only around the early 2000s. The green chemical methods, which are even more recent, have shown to exhibit a good potential and there is more scope of development and exploration in this field. In the near future, such methods will pave the path for a larger scale of study and applications of diamondoids in daily human life.

Author Biography

Dr. Shiladitya Banerjee completed his Bachelors (with Honors) in Chemistry from Presidency College, Kolkata in 2007 and Masters in Chemistry from Indian Institute of Technology, Bombay in 2009. He pursued his Ph.D. in Theoretical and Computational Chemistry from the University of Potsdam, Germany from 2010-2014 and post-doctoral research in the Council of National Research and Scuola Normale Superiore in Pisa, Italy from 2015-2018. During his Ph.D. and postdoctoral work, Dr. Banerjee worked on different aspects of diamondoids and published multiple articles in peer-reviewed journals. Since 2020, he is working as an Assistant Professor in the department of Chemistry in Midnapore College (Autonomous), India.

References

1. Yeung, K. W., Dong, Y., Chen, L., Tang, C. Y., Law, W. C., Pong, G. C., *Nanotechnology Reviews,* **2020**, 9(1), 650-669
2. Landa S., Machacek, V., *Collect Czech Chem. Commun.,* **1933**, 5, 1-5
3. Maung, K., Earthman, J. C., Mohamed, F. A., *Acta Matter*, **2012**, 60, 5850-5857
4. Zhou, F., Lee, J., Dallek, S., Lavernia, E. J., *J. Mater. Res*., **2001**, 16, 3451-3458
5. Clay, W. A., Dahl, J. E. P., Carlson, R. M., Shen, Z., *Rep. Prog. Phys*., **2015**, 78, 016501
6. Landt, L., Bostedt, C., Walter, T., Möller, T., Dahl, J. E. P., Carlson, R. M. K., Tkachenko, B. A., Fokin, A. A., Schreiner, P. R., Kulesza, A., Mitric, R., Bonacic-Koutecký, V., *J. Chem. Phys*., **2010**, 132, 144305 (1-6)
7. Weigel III, W. K, Dang, H. T., Feceu, A., Martin, D. B. C. *Org. Biomol. Chem.,* **2022**, 10, 20-36
8. Gunawan, M. A., Hierso, J. C., Poinsot, D., Fokin, A. A., Fokina, N. A., Tkachenko, B. A., Schreiner, P. R., *New J. Chem.***, 2014**, 38, 28-41
9. Wingert, S.W., *Fuel.***, 1992**, 71, 37-43

10. Katz, B. J., Mancini, E. A., Kitchka, A. A., *AAPG Bull*, **2008**, 92, 549-556
11. Jinggui, L., Philip, P., Mingzhong, C., *Org. Geochem*., **2000**, 31, 267-272
12. Akinlua, A., Jochmann, M. A., Lorenzo-Parodi, N., Stojanovic, N., Kaziur, W., Liu, S., Schmidt, .TC., *Analytica Chimica Acta*, **2019**, 1091, 23-29
13. Alic, J., Stolar, T., Stefanic, Z., Uzarevic, K., Sekutor, M.,*ACSSustainable Chem. Eng*., **2023**, 11, 2, 617-624
14. Alic, J., Biljan, I., Stefanic, Z., Sekutor, M.,*Nanotechnology*, **2022**, 33, 355603-355614

NH_4^+ ION TEMPLATED SELF-ASSEMBLY IN CU(II) COMPLEX OF NTA: SYNTHESIS, STRUCTURE AND HIRSHFELD SURFACE ANALYSIS

Prankrishna Manna*[,a], Ritam Das[a] and Subrata Mukhopadhyay[,b]

[a] Department of Chemistry, Midnapore City College, Kuturiya, Bhadutala, Midnapore, West Bengal 721129
[b]Department of Chemistry, Jadavpur University, Kolkata-32
*Corresponding author *Email: prankrishna_manna@yahoo.com*

Abstract

Molecular self-assembly is the key process for functioning of biological systems. During last decades scientists have become much more aware that for understanding the micro and nano-scale processes as well as for controlled molecular or atomic organization at these length scales mastery over the naturally occurring self-assembly process is the only solution. In this regard, we discuss the self-organizing role of the ammonium ion in the solid-state organization of a Cu(II) complex of urotropin and nitrilo-triacetic acid. We discuss various aspects of this spontaneous assembly, especially the role of relative sizes of various components that take part in the assembly. Due to the disproportionate size of the three dimensional (3D) ammonium ion template and the Cu(II) complex, the 3D nature of template is masked by the comparatively bigger meal-organic complex, resulting a 2D self-assembled superstructure.

Keywords: Cu(II) complex, self-assembly, NH_4^+ ion template, water topology, Hirshfeld Surface Analysis.

Introduction:

Directed self-assembly of simple molecular components into poly-molecular architecture of increasing complexity is the main theme of supramolecular synthesis.[1] Various non-covalent binding modes determine the distinct level of structural complexity. Non-covalent nature of inter-component binding renders supramolecular assembly a dynamic character which allows self-sorting through molecular recognition, a property inherent to biological systems.[2] Template directed assembly is at present a powerful supramolecular synthetic strategy and a diverse range of network solids have been targeted and successfully synthesized [3] using this approach. In the present communication we report the unusual templating action of NH_4^+ ions which gives rise to extended hydrogen bonded self-assembled 2D layers of $[Cu(II)(NTA)(HTM)]^-$ units which are supported by an unprecedented sefl-organized water ribbons of successive cyclic water hexamers and tetramers joined at the corners with a flip-flop topology.

Synthesis of Complex:

Copper(II) chloride hexahydrate (0.242 g, 1.0 mmol) dissolved in water (25 mL) was treated with nitrilotriacetic acid (0.382 g, 2.0 mmol) in water (25 mL) at 60 °C to give a clear blue colour solution. A warm aqueous solution (20 mL) of urotropine (0.280 g, 2.0 mmol) was added dropwise to the above solution and the pH of solution is adjusted to 6.5- 7.5 by adding ammonium hydroxide solution dropwise. After a few weeks, blue colour single crystals suitable for X-ray analysis were obtained.

X-ray Crystallographic

Single crystal X-ray diffraction intensity data of Cu(II) complex were collected at 150(2) K using a Bruker APEX-II CCD diffractometer equipped with graphite monochromated Mo Kα radiation (λ = 0.71073 Å). Data reduction was carried out using the program Bruker SAINT. [4]

Hirshfeld surface analysis

The Hirshfeld surface [8,9] is defined based on a stockholder portioning scheme where the contribution of the respective molecule to the overall crystal electron density is greater than 50% at every point inside the surface. The Hirshfeld surfaces were calculated using CrystalExplorer 3.0.

Crystal Structure Description

Single crystal X-ray crystallographic study reveals that the mononuclear Cu(II) complex is constituted by mono-coordinated Urotropin and triply coordinated NTA molecules. The asymmetric unit [Fig 1] also contains an amonioun ion and four solvent water molecules (not shown in the figure). Cu(II) is having a relatively less common trigonal bi-prismatic coordination environment with three oxygen atoms (O1, O3 and O5) of NTA occupying the basal plane and two nitrogen atoms (N1 of NTA and N5 of Urotopin) occupying the trans axial coordination sites. Cu-O distances in the basal plane span a narrow range [(1.9980(17) – 2.1234(16) Å] and the two axial Cu-N distances are 1.9805(18) [Cu1-N2] and 1.9952(18) Å [Cu1-N1] respectively.

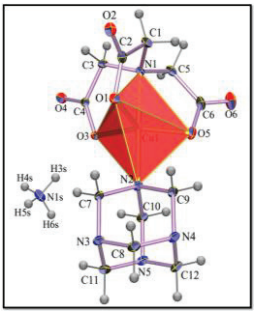

Fig 1: ORTEP diagram (30% ellipsoidal probability) with atom numbering scheme. Solvent water molecules have been omitted for clarity.

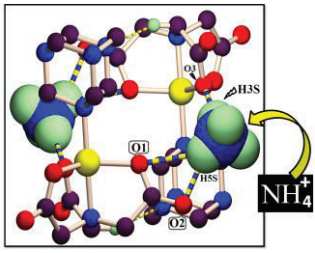

Fig 2: The ammonium ion assisted supramolecular dimer of Cu-NTA-Urotropin mono nuclear units.

The self-organized super structure of the compound can be regarded as the four level hierarchical assemblies of component building blocks into a hydrogen bonded network having pillar-layered architecture. At the lowest level the coordinative forces lead to $[Cu(II)(NTA)(HTM)]^-$ anionic complexes. In the next higher level ion pair formation among two of the above mentioned anionic units and two NH_4^+ cations lead to the hydrogen bonded self-organized centrosymmetric dimeric units shown in Fig 2. Main force organizing this dimeric unit is the strong NH···O hydrogen bond between carboxylate groups of NTA and ammonium cations. A weaker CH···N hydrogen bond also operates in unison in which N3 nitrogen of Urotopine acts as acceptor for hydrogen donated by -CH group of NTA .

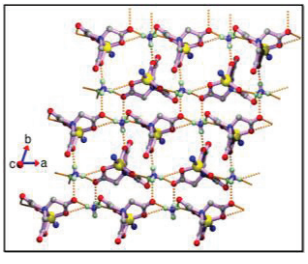

Fig 3: The ammonium ion template supramolecular layer of Cu-NTA-Urotropin mono nuclear units in the *ab* plane. Urotopine moiety omitted for clarity.

Tetrahedral geometry of the ammonium cation and its relatively samller size compared to the $[Cu(II)(NTA)(HTM)]^-$ anionic complexe are the two important factors for this particular self-organized superstrcutre. Two of the fours hydrogens of the ammonium ions (H3S and H5S) is responsible for this cyclic dimeric units. H5S simultaneously act as double donor for O1 and O2 atoms due to the formation of bifurcated hydrogen bonding and H3S act as unique donor for O3 atom. Both the samller size of amion ion and tetrahedral disposition of H3S and H5S helps this assembly. Other two hydrogen atoms of the ammonium ions (H4S and H6S) are tetrahedrally disposed away from this centric dimeric unit and as a result of this geometric arrangement successive dimeric units are integrated into a layered structure (*ab* plane) as has been depicted in Fig 3.

This integration is again enforced by similar bifurcated hydrogen bonding between H6S and O5, O6 carboxylate O atoms of NTA and a single hydrogen bond between H4S and O2. In this hydrogen bonded supramolecular layer, each of the ammonium ions act as template for the self-assembly where the tetrahedral disposition of the four hydrogen atoms around the ammonium ion leads to organization of four $[Cu(II)(NTA)(HTM)]^-$ anionic complexes around each amonioum ion Fig 4. Though tetrahedral geometry generally gives rise to three dimension networks, in the present case the disparity in sizes between ammonium cations and $[Cu(II)(NTA)(HTM)]^-$ complex anionis leads to a 2D assembly where smaller ammonium cations are pocketed around four anions thus forming two bifurcated hydrogen bond and two single hydrogen bonds.

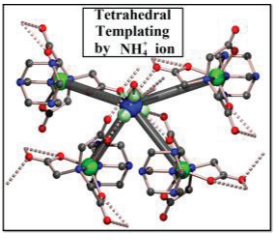

Fig 4: Tetrahedral templation by NH_4^+ ion. Dotted lines indicate hydrogen bonding. Gray cylinders have been used to help visualize tetrahedral templation and are not any real bond

In the fourth level of the hierarchy solvent water molecules which organize in a particular way to slef-assemble in the form of water ribbons, support successive hydrogen bonded neutral layers mentioned in the previous section [Fig 5]. The self-organized water structure found here is a new one dimensional polymeric water motif of planar cyclic water hexamers and tetramers [Fig 5]. Successive water tetramer and hexamer motifs are joined at the corner through the sharing a common water molecule and has a spirocyclic topology in which respective planes are rotated with respect to each other. This type of spirocyclic topology has been reported previously for 1D water polymer consisting only of either water tetramesr or water hexamers. The average O····O separation in the present case is 2.88Å [Fig 6(a)]. Unfortunately the complete hydrogen bonding pattern of the ribbon could not be determined as sever disorder in oxygen atom positions did not allow us to locate the position of the hydrogen atoms. To gain more insight into the nature of the water-chain we have computed the optimized geometry of the corner-shared water hexamer and tetramer which is the basic building block of the polymeric water chain with the initial geometry form taken from the observed motif in the crystal structure. Initial hydrogen atom positions of water oxygen atoms were calculated manually. The calculations have been performed both at the DFT level and at the Hartree-Fock level. The calculated O····O distances have been depicted in Fig 6(b).

The pillaring action of the flip-flop water chain of water hexamer and tetramer that has been observed in the present structure is nearly identical to that of similar role

played by a flip-flop water tetramer only motif reported previously by us. In the observed water chain, water molecules besides forming hydrogen bonding within themselves, establish hydrogen bonding contacts with the supramolecular metal-organic layer by forming hydrogen bonding with the NTA oxygen atoms and the ammonium hydrogen atoms gaining additional support from the organic components.

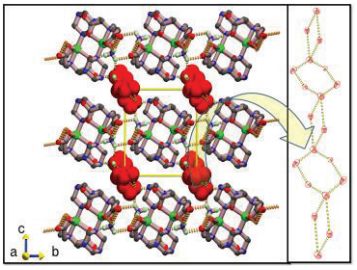

Fig 5: Water tape supported supramolecular layers.

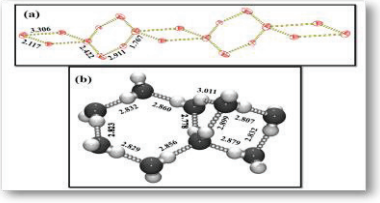

Fig 6. (a) The topology of the water tape consisting of cornered-shared hexamers and tetramers as observed in **1**. (b) The computed optimized geometry of the basic unit of the polymeric water chain by DFT method.

Hirshfeld surface analysis

Hirshfeld surfaces [8,9] and the associated 2D-fingerprint[11] plots were calculated using CrystalExplorer,[10] which accepts a structure input file in CIF format. Bond lengths to hydrogen atoms were set to typical neutron values (C–H = 1.083 A, N–H = 1.009 A). For each point on the Hirshfeld isosurface, two nucleus external to the surface, and d_i, the distance to the nearest nucleus internal to the surface, are defined. The normalized contact distance (d_{norm}) based on d_e and d_i is given by

$$d_{\text{norm}} = \left| \frac{d_i - r_i^{\text{vdw}}}{r_i^{\text{vdw}}} + \frac{d_e - r_e^{\text{vdw}}}{r_e^{\text{vdw}}} \right| \qquad (1)$$

where r_i^{vdW} and r_e^{vdW} are the van der Waals radii of the atoms. The value of d_{norm} is negative or positive depending on intermolecular contacts being shorter or longer than the van der Waals separations. The parameter d_{norm} displays a surface with a red-white-blue color scheme, where bright red spots highlight shorter contacts, white areas

represent contacts around the van der Waals separation, and blue regions are devoid of close contacts. The Hirshfeld surfaces of the title complex were analyzed to illuminate the nature of the intermolecular interactions and are illustrated in Fig. 9 showing the surfaces that have been mapped over d_e, d_{norm}, shape-index and curvedness and H-bonding interaction in molecular Hirshfeld surfaces (right).

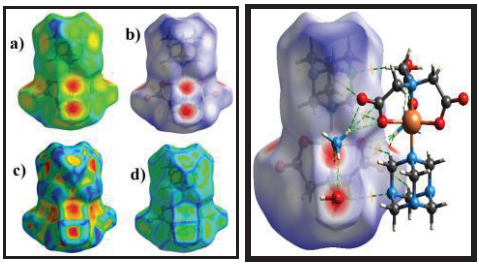

Fig 7. Hirshfeld surfaces mapped with a) d_e; b) d_{norm}; c) shape-index and d) curvedness for the title complex 1(left) and H-bonding interaction in molecular Hirshfeld surfaces (right).

As expected, the d_{norm} surfaces of Fig. 7 reveal the close contacts of hydrogen bond donors and acceptors, but other close contacts are also evident. In d_{norm} surfaces, the large circular depressions (deep red) are the indicators of hydrogen bonding contacts whereas other visible spots are due to H····H contacts. The dominant H····O interactions in the title crystal structure are evident in the Hirshfeld surface plots by the bright red area (Fig 7) and light red spots are due to C–H····O interactions. The shape-index and curvedness surfaces have been shown to convey the information about each donor–acceptor pair and to measure how much shape effectively divides the surfaces into sets of patches, respectively. The tiny extent of area and light color on the surface indicates weaker and longer contacts other than hydrogen bonds. The leading interactions are visible on the Hirshfeld surfaces as well as in the fingerprint plots (Fig. 8), where one molecule acts as a donor (de > di) and the other as an acceptor (di < de). These fingerprint plots are quite asymmetric, because the interactions occur between two chemically and crystallographically distinct molecules. The intermolecular interactions concerned in the structure appear as distinct spikes in the fingerprint plot and the proportions of individual interactions have been mentioned in Fig. 8.

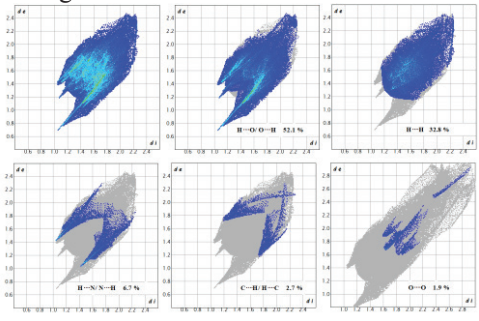

Fig 8. Fingerprint plots: full (upper left) and resolved into different intermolecular interactions within the title complex showing percentages of contacts contributing to the total Hirshfeld surface area of the molecules.

Fig. 9 contains the percentages of contributions for a variety of contacts in the title crystal structure. This quantitative conclusion is further evident from the shape of the blue outline on the curvedness surface (Fig. 9), which unambiguously delineates contacting patches of the molecules. The Hirshfeld surfaces certainly allow a much more detailed scrutiny by displaying all the intermolecular interactions within the crystal and this methodology has very important promise in crystal engineering.

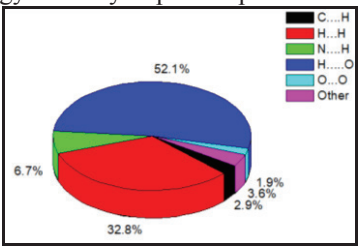

Fig 9. Relative contributions of various intermolecular contacts to the Hirshfeld surface area of complex 1.

Conclusion:

In summary we have synthesized a copper complex of NTA and Urotopin which in which the ammonium cations have played very important role in the supramolecular organization of the anionic complexes by acting as templates for the hydrogen bonded two dimensional layered assemblies. Considering the rarity of the cationic templates the present complex is a interesting one which shows how the geometric nature and the size of the cation can lead to interesting supramolecular self-assembly. The solvent water molecules also organize themselves in a unique manner with an unprecedented 1D water motif of water hexamer and water tetramer with spirocyclic topoly that supports the host supramolecular layers by acting as pillars.

References:

1. Lin N, Langner A, Tait SL., Rajadurai C, Ruben M, Kern K, Chem. Commun.: Template-directed supramolecular self-assembly of coordination dumbbells at surfaces, 2007, 4860–4862.
2. (a) Heather MC, Stephanie CC, Lubbe van der, Hetherington K, Minard A, Pask C, Howard MJ, Guerra CF, Wilson AJ., *Chem. Eur. J.* Supramolecular Self-Sorting Networks using Hydrogen-Bonding Motifs, 2019, 25, 785 – 795. (b) Durham, ACH. Klug, A. Nat. N. Biol.: Mechanism of self-assembly of tobacco mosaic virus protein: Nucleation-controlled kinetics of polymerization, 229, 42–46.

3. (a) Diederich F, Stang PJ, Templated Organic Synthesis , Wiley-VCH, 2000. (b) Lo P K, Sleiman HF, J. Am. Chem. Soc., Nucleobase-templated polymerization: copying the chain length and polydispersity of living polymers into conjugated polymers, 2009, **131** , 4182. (c) Bhattacharyya T, Panda D, Dash J, Org. Lett.: Supramolecular Template-Directed In Situ Click Chemistry: A Bioinspired Approach to Synthesize G-Quadruplex DNA Ligands, 2021, 23, 3004−3009.
4. Bruker SAINT, version 6.36a; Bruker-AXS Inc.: Madison, Wisconsin, 2002.
5. Bruker SMART, version 5.625 and SADABS, version 2.03a; Bruker AXS Inc.: Madison, Wisconsin, 2001.
6. Sheldrick GM, Acta Crystallogr., Sect. A : Crystal structure refinement with SHELXL 2008, 64, 112−122.
7. Spek, A. L. PLATON, Molecular Geometry Program. J. Appl. Crystallogr. Single-crystal structure validation with the program PLATON, 2003, 36, 7−13.
8. Seth SK, Saha I, Estarellas C, Frontera A, Kar T, Mukhopadhyay S, Cryst. Growth Des.: Supramolecular Self-Assembly of M-IDA Complexes Involving Lone-Pair···π Interactions: Crystal Structures, Hirshfeld Surface Analysis, and DFT Calculations [H_2IDA = iminodiacetic acid, M = Cu(II), Ni(II)], 2011, 11, 3250–3265.

CONJUGATED POLYMER FOR SENSING METAL ION

Sk Najmul Islam

Department of Chemistry, Midnapore College (Autonomous), Midnapore- 721101, West Bengal.
E-mail: sknajmul.islam@midnaporecollege.ac.in

Abstract

Conjugated polymer having triazole spacer has a great interest in recent days for detection of heavy transition metal ions. Great effort has recently been devoted to the design and construction of molecular sensory systems for a broad range of environmental and biological analytes. A sensor is defined as "a device that detects or measures a physical property and records, indicates or otherwise response to it." A sensor achieves this goal by responding to an external stimulus and converting it into a signal which can be measured or recorded.

Introduction

A sensor device carries three elements: a receptor, a signal transducer and a read out(fig. 1). [1-4] The receptor should have the ability to discriminate and bind a specific target substances known as analyte . Successful ,receptor- analyte complex formation depends on the size, shape and binding energy of the receptor and analyte molecules. Signal transduction is the process through which an interaction of receptor with analyte results a measurable form of energy change and is transformed to a signal change that can be read and quantified . The read out domain is the part responsible for describing the binding event.[5-7]

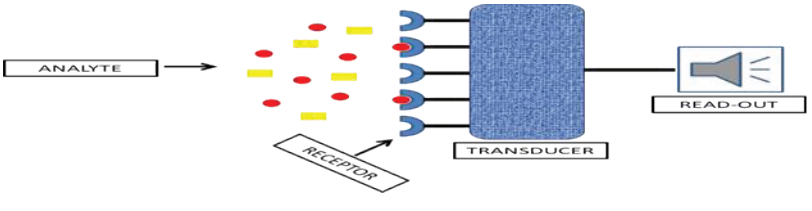

Fig. 1. Schematic diagram of a sensor device (especially a chemical sensor device)

A chemical sensor is a device that qualitatively or quantitatively recognize the presence of specific chemical substances, a class of chemicals or a specific chemical reaction. This field of chemical sensing depends upon novel materials .Polymers, crystals, glasses, particles and nanostructures have made a profound impact and have endowed modern sensory systems with superior performance.[8]

Mechanism

Among them conjugated polymers (CPs) offer a innumerable opportunities to couple analyte receptor interaction, into observable (transducible) responses. A key advantage of CP based sensors over devices using small (chemosensor) elements is the potential to exhibit collective properties that are sensitive to very minor perturbation which is shown in fig.2. In particular the CP's transport properties, electrical conductivity or rate of energy migration, provide amplified sensitivity.[9]

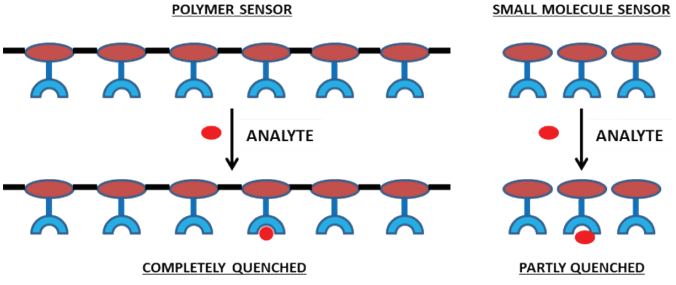

Fig. 2. Small molecule sensor vs conjugated polymer sensor

CP based sensors have been formulated in a variety of schemes. Conductometric sensors display changes in electrical conductivity in response to an analyte interaction.[10-12] Potentiometric sensors relay on analyte- induced changes in the system's chemical potential.[13] Colorimetric sensors refer to change in a material's absorption properties. Fluorescence sensors is based upon changes in intensity, energy transfer, wavelength (excitation and emission) and lifetime.[14-15]

Among all of the above schemes fluorescence quenching is a widely used and rapidly expanding method in chemical sensing due to carrying some important features. An important feature of the fluorescent chemo sensors is that signal transduction of the analytes binding event into a readout can happen in a very short time and without any other assistance.[1] This makes real time and real space detection of the analyte possible as well as imaging associated with analyte distribution. Fluorescence quenching is often achieved through photoinduced electron transfer (fluorescence "turn on" or "turn off") mechanism as depicted in fig.3 & fig.4.[16-18]

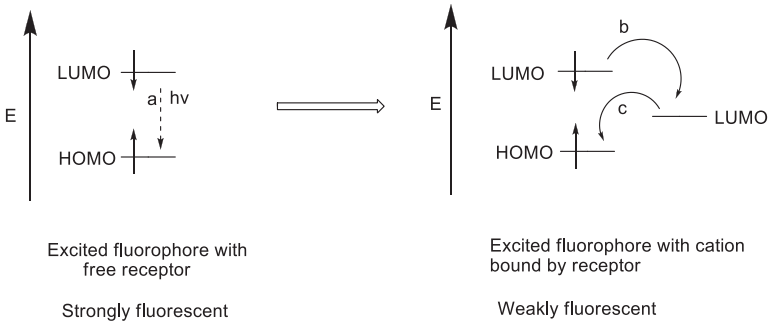

Fig.3. Orbital energy diagram for fluorescence "turn off" PET sensors before and after binding cation (a) fluorescence emission (b) forward electron transfer (c) backward electron transfer.

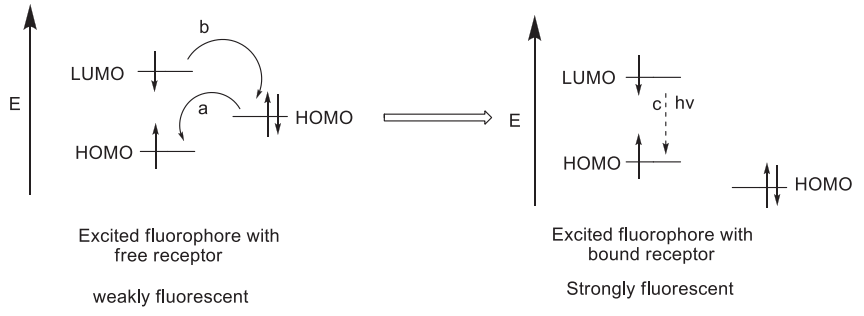

Fig.4. Orbital energy diagram for fluorescence "turn on" PET sensors before and after binding cation (a) forward electeron transfer (b) backward electron transfer (c) fluorescence emission.

Heavy metal ions can disturb normal biological functions and stimulate cellular stress responses. Some examples are given below.[19]
Zinc plays an important role in neurophysiology, inducing the formation of β-amyloid that is related to Alzheimer's disease.[20]Excess zinc in the brain has been implicated in neuropathology. Zinc release also contributes to hypoglycemia-induced neuronal death.[21] Mercury can induce aberrations in microtubules, ion channels, and mitochondria.[22] Lead is poisonous to animals and humans ,damaging the nervous system and causing brain disorders and excessive lead also cause blood disorders in mammals. Inhalation of cadmium containing fumes can result initially in metal fume fever but may progress to chemical pnenmanitis, pulmonary edema and death.

Therefore a metal sensing molecule is quite desirable for biological studies and for diagnosis of certain disease. And we are interested in the development of highly sensitive and selective chemo sensor materials for the detection of metal ions in environmental or biological systems . In particular, many attempts have focused on the design of sensing systems with unique optical properties as output signals that provide real time monitoring capabilities. Preparation and utilization of small

molecules that show selective binding to the target metal ion constitute one practical route towards this goal. But many of these probes suffer from one more limitations, including irreversibility, slow response, low selectivity and sensitivity.

In last two decades conjugated polymer fluorescent sensors for heavy and transition metal ions have attracted much interest owing to their high sensitivity, selectivity, rapidity and ease of measurement. Their excellent sensitivity is attributed to sensory signal amplification that originates from energy migration along the conjugated backbone upon light upon light excitation.

Application

There is different type of molecules based conjugated polymers for sensing of metal ions. Among them fluorene is one of the most universally employed building blocks in constructing conjugated copolymer for metal ion sensing that show light emitting characteristics. Some literature reported fluorene based conjugated polymers for metal ion sensing are given below fig.

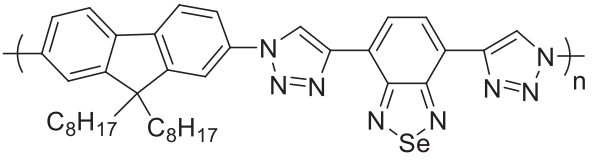

Fig. 5. Fluorene & benzochalcogendiazole based conjugated polymer fluorescence sensor for Ni^{2+} ion detection.

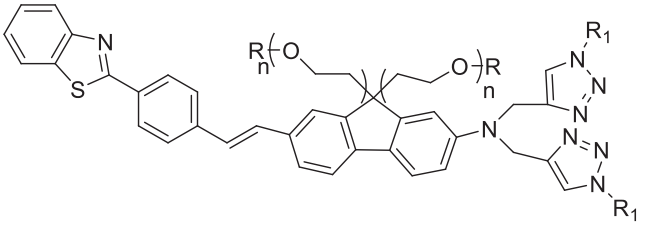

P1 ⟶ $R=C_2H_5, R_1=n\text{-}C_4H_9$

P2 ⟶ $R=C_2H_5, R_1=n\text{-}C_{11}H_{22}SH$

P3 ⟶ $R=CH_3, R_1=C_{11}H_{22}SH$

Fig. 6. Hydrophilic 1, 2, 3-triazolyl fluorene based polymers for detection of Zn^{2+} and Hg^{2+} ion.

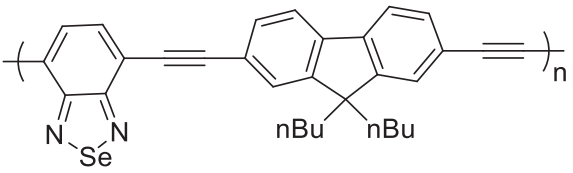

Fig. 7. Fluorene and benzoselenodiazole based conjugated polymer for Hg^{2+} ion detection.

Conclusion

From the literature study we conclude that the copper catalyzed azide alkyne cycloaddition reaction has an enormous impact on the field of polymer science because of its high efficiency, mild condition and technical simplicity. The click formed triazole can be used as a metal binding ligand and it is more than a simple linker group.

Reference

1. Jenkins TF, Leggett DC, Ranney TA. Vapor signatures from miltary explosives, part 1: Vapor transport from buried military-grade TNT.
2. Czarnik AW. A sense for landmines. Nature. 1998 Jul 30;394(6692):417-8.
3. Salinas Y, Martínez-Máñez R, Marcos MD, Sancenón F, Costero AM, Parra M, Gil S. Optical chemosensors and reagents to detect explosives. Chemical Society Reviews. 2012;41(3):1261-96.
4. Salinas Y, Martínez-Máñez R, Marcos MD, Sancenón F, Costero AM, Parra M, Gil S. Optical chemosensors and reagents to detect explosives. Chemical Society Reviews. 2012;41(3):1261-96.
5. Moore DS. Instrumentation for trace detection of high explosives. Review of Scientific Instruments. 2004 Aug 1;75(8):2499-512.
6. Walsh ME. Determination of nitroaromatic, nitramine, and nitrate ester explosives in soil by gas chromatography and an electron capture detector. Talanta. 2001 May 10;54(3):427-38.
7. Smedts BR, Baeyens W, De Bisschop HC. Separation of arsines and trinitrotoluene by reversed phase high performance liquid chromatography and micellar electrokinetic capillary chromatography. Analytica chimica acta. 2003 Oct 24;495(1-2):239-47.
8. Babaee S, Beiraghi A. Micellar extraction and high performance liquid chromatography-ultra violet determination of some explosives in water samples. Analytica chimica acta. 2010 Mar 3;662(1):9-13.
9. Eiceman GA, Stone JA. Peer reviewed: ion mobility spectrometers in national defense.
10. Najarro M, Morris ME, Staymates ME, Fletcher R, Gillen G. Optimized thermal desorption for improved sensitivity in trace explosives detection by ion mobility spectrometry. Analyst. 2012;137(11):2614-22.

11. Hallowell SF. Screening people for illicit substances: a survey of current portal technology. Talanta. 2001 May 10;54(3):447-58.
12. Zhang HX, Hu JS, Yan CJ, Jiang L, Wan LJ. Functionalized carbon nanotubes as sensitive materials for electrochemical detection of ultra-trace 2, 4, 6-trinitrotoluene. Physical Chemistry Chemical Physics. 2006;8(30):3567-72.
13. Krausa M, Schorb K. Trace detection of 2, 4, 6-trinitrotoluene in the gaseous phase by cyclic voltammetry. Journal of electroanalytical chemistry. 1999 Jan 29;461(1-2):10-3.
14. Riskin M, Tel-Vered R, Bourenko T, Granot E, Willner I. Imprinting of molecular recognition sites through electropolymerization of functionalized Au nanoparticles: development of an electrochemical TNT sensor based on π-donor− acceptor interactions. Journal of the American Chemical Society. 2008 Jul 30;130(30):9726-33.
15. Shanmugaraju S, Joshi SA, Mukherjee PS. Fluorescence and visual sensing of nitroaromatic explosives using electron rich discrete fluorophores. Journal of Materials Chemistry. 2011;21(25):9130-8.
16. Kumar S, Venkatramaiah N, Patil S. Fluoranthene based derivatives for detection of trace explosive nitroaromatics. The Journal of Physical Chemistry C. 2013 Apr 11;117(14):7236-45.
17. Kaur S, Bhalla V, Vij V, Kumar M. Fluorescent aggregates of hetero-oligophenylene derivative as “no quenching” probe for detection of picric acid at femtogram level. Journal of Materials Chemistry C. 2014;2(20):3936-41.
18. Roy B, Bar AK, Gole B, Mukherjee PS. Fluorescent tris-imidazolium sensors for picric acid explosive. The Journal of Organic Chemistry. 2013 Feb 1;78(3):1306-10.
19. Kartha KK, Babu SS, Srinivasan S, Ajayaghosh A. Attogram sensing of trinitrotoluene with a self-assembled molecular gelator. Journal of the american chemical society. 2012 Mar 14;134(10):4834-41.
20. Gole B, Bar AK, Mukherjee PS. Fluorescent metal–organic framework for selective sensing of nitroaromatic explosives. Chemical Communications. 2011;47(44):12137-9.
21. Gong YN, Jiang L, Lu TB. A highly stable dynamic fluorescent metal–organic framework for selective sensing of nitroaromatic explosives. Chemical Communications. 2013;49(94):11113-5.
22. Huang XL, Liu L, Gao ML, Han ZB. A luminescent metal–organic framework for highly selective sensing of nitrobenzene and aniline. RSC advances. 2016;6(91):87945-9.

SOLVENT FREE ORGANIC SYNTHESIS TECHNIQUES: AN IMPORTANT APPROACH FOR GREEN CHEMISTRY

Dr. Chhabi Garai
Assistant Professor, Department of Chemistry, Pingla Thana Mahavidyalaya
Email: chhabi.garai@gmail.com

Abstract:

Solvents are most important part to carry out any chemical reaction. But unfortunately most of solvents utilized in chemistry laboratory or industries are toxic and hazardous in nature which causes serious risk and health effect on environment as well as human being. To avoid or reduce such toxic effects must needed another pathway where eliminate the use of hazardous solvents. This is one of the purposes of green chemistry. Therefore, the principle factor for the green approaches of organic reactions is utilization of renewable starting material, non toxic chemicals and performed in solvent free condition. In this paper I have tried to highlight the advantages of solvent less techniques and different techniques utilized to perform solvent free reactions with examples.

Key words: Organic synthesis, green chemistry, solvent free condition, microwave irradiation, ultrasound irradiation, photo-chemical reaction

Introduction:

Solvents are not only important to perform a chemical reaction but it plays a giant role in our daily life and necessary for several applications like cleaning, coating, separation etc. However, most of them have negative impacts on the environment because they are responsible for ozone layer depletion or tropospheric smog formation. Again some of them are neurotoxin, carcinogen, hepatotoxin etc. and causes several health effects like stertility or even caner. Solvents mainly can harm the human body through eyes, blood, skin, kidneys and lung. Hence utilization of solvents is strictly prohibited for the environmental and health issues . Any one of the organic solvents is not safe, only difference is some of them are more toxic and others are less toxic. Few examples solvents with their toxicities for health effect are provided in table 1 and it has been obvious that aromatic hydrocarbon solvents are more toxic and volatile.

Table 1: Some of the dangerous health effects resulting from solvents

Health Hazard	Solvent that causes the hazard
Carcinogen	Ethylene dichloride, methylene chloride, dioxin, chloroform, perchloroethane.
Toxic	Xylene, benzene, toluene
Irritant	Ammonium solution
Hepatotoxin	Dioxane, acetonitrile, carbon tetrachloride, phenol
Nurotoxin	Cresol, methylene chloride, xylene, carbon disulfide
Nephrotoxin	Ethylenediamine, chlorobenzene, dioxane, acetonitrile, Allyl alcohol, hexachloronaphthalene, phenol

Even incorrect storage of solvents may causes fires or explosion. The major problem of utilization of solvent is the time consuming heating and recovery of the solvents after reaction completion.

Therefore, the pollution prevention Act of 1990 of environmental protection agency (U.S.EPA) encouraged utilizing novel techniques to reduce or eliminate toxic pollutants or wastes to protect the natural environment. For this reason researchers are made great efforts for the few decades to develop novel synthetic strategies to eliminate hazardous solvents or to use safer solvents. From this aspect solvent free reactions are most promising to solve the earlier stated problems. Advantages of solvent free reactions and solvent free reaction techniques with examples are discussed here.

Advantages of solvent free reaction: Solvent less reaction techniques is an important approach towards green chemistry to build up a sustainable and pollution free environment. There are various advantages of this technique (figure 1)such as (i) Reduce pollution for avoiding toxic solvents, (ii) Low costs, (iii) Simple process as there is no solvent separation or purification (iv) Easy to handling, (v) Eco- friendly and (vi) Reduced reaction time.

Solvent free organic reaction techniques: There are several examples of various types of organic reactions carried out under solvent free condition in literature. These reactions have performed via different techniques. Among these techniques grinding in a mortar is the oldest method. Recent time the manual grinding has been developed to automated methods like grinding by rotating mortar or high speed ball milling. Except this other techniques like microwave irradiation, ultrasonic irradiation or performance under photochemical condition are exploited to precede solvent free reactions.

Mechanochemistry: The term 'mechanochemistry' is generally utilized to express those chemical reactions which are depends on mechanical force as source of energy. This technique is subdivided into two methods grinding and high speed ball milling process.

Grinding mode synthesis: In organic synthesis, grinding method has been used frequently in comparison to traditional method. In this method reactions are precede by the local heat generated through friction from the grinding of substance and reagent taken in a mortar. Various types of organic reactions such as Reformatsky reaction, Knovenegal reaction, Micheal addition, Dieckmann condensation, phenol coupling reactions etc. are reported.
1,5 diketone prepared by Micheal addition utilizing eco-friendly method mechanochemistry where the reactants are grinding together in mortar.

Another reaction reduction of carbonyl compounds utilizing $NaBH_4$ carried out under solvent free condition by this method.[3]
High speed ball milling: Extensive research on performance of solvent free reaction techniques utilizing catalytic amount of catalyst instead of stoichometric amount has developed high speed ball milling method which can lead to the reduced amount of catalyst loading, a shorter reaction time, and higher yield. For example, N-hetrocyclic compounds are prepared from Schiff bases of aldehyde or ketones and amines under solvent free condition in presence of manganese(III) acetate as catalyst. [3]

Another example is synthesis of amides from C-H bonds by reaction with azides in presence of different catalysts (scheme 4) which is carried out through this technique. [2]

Solvent less reaction under microwave irradiation: Newly developed synthetic technique to carry out organic reactions under microwave irradiation known as microwave assisted organic synthesis is a novel approach for green chemistry. This is because; the synthesis process through this technique is very easy, quick, clean and affordable. The advantage of this technique is that the reaction proceeds with faster rate and completed in very short time with improved yield compared to traditional methods. In this process high frequency electromagnetic radiations used in microwave ovens to heat the reaction mixture via dipolar Polarization or ionic conduction. The main difference between conventional heating and microwave is the even distribution of heat and higher reaction rate in absence of solvents.

The microwave-assisted synthesis imidazole from α-diketone (Scheme 5) is achieved in a short period of time (10 mins) in presence of basic alumina giving excellent yield under microwave condition but in traditional method the reaction takes 4 hours for completion in presence of acetic acid as solvent.[3]
Oxidation of alcohols to ketones under solvent free microwave irradiation in presence of MnO2-silica completed within a minute.[3]

C-C coupling reaction has been carried out under solvent free microwave irradiation in presence of catalyst which is easy, safe and simple.[2]

Solvent less reaction under ultrasound irradiation: Recently developed another technique to carried out solvent less reaction is ultrasound assisted synthesis where ultrasonic lowers the reaction temperature, proceed at faster rate in ambient settings. Here also observed similar advantages such as shorter reaction time, high yield, milder reaction condition and simple process as like microwave assisted organic synthesis. There are several reports in literature on organic synthesis via this process.
N-alkylated amines are prepared from benzyl halides using eco-friendly method in presence of ultrasonic waves. This reaction occurs through two steps, at first halide is oxidized to aldehyde by N-methylmorpholine N-oxide (NMO), followed by direct reductive amination with amines using sodium borohydride and montmorillonite K-10 catalyst as the reducing system.
Another example is the preparation of 3-carboxycoumarin by condensation of substituted benzaldehydes and Meldrum's acid was done in water using catalytic amounts of zirconium oxide chloride under ultrasound irradiation.[3]
Solventless photochemical reaction: Performance of chemical reaction utilizing light as a source of energy has grown interest in recent years due to availability of efficient light source which are cheap, with precise wavelength and quite powerful. Photochemical reactions are preceding in milder condition and ambient temperature compared to traditional methods. There are several reactions which occurs in presence only light not at thermal condition. Various types of reactions can be carried out with only light and without the need for solvents, such as polymerization, dimerization, and cyclization.[2]
Another example is synthesis of imidazole pyridines and imidazole thiazoles under solvent-free conditions and without the need for a catalyst, using only visible light as an activator.[7]

Similarly thioacetals of benzaldehyde are synthesized in presence of Eosyn Y as catalyst and blue LED light as a source of energy with the yield more than 99%. [7]

Conclusion:

The main aim of green chemistry is the building of a pollution free sustainable environment by using safer materials which not causes any type of health effects. Therefore, avoiding of toxic solvents in laboratory as well as industries is the best policy. Solvent free organic synthesis methodology is an important approach

towards green chemistry where toxic volatile solvents are eliminated and also reduces cost, gives better yield and saves times. Again the utilization of alternative energy sources like microwave irradiation, ultrasonic irradiation even natural energy sources (photochemical) to collect the activation energy makes the techniques as green process. In this paper I have discussed different methodologies utilized to carried out solvent free organic synthesis with examples.

References:

1. Tong R, Zhang L, Yang X, Liu J, Zhou P, Li J. Emission characteristics and probabilistic health risk of volatile organic compounds from solvents in wooden furniture manufacturing. J Clean Prod. 2019 Jan;208:1096–108.
2. Younis A, Said AO, Solvent-free Organic Reaction Techniques as an Approach for Green Chemistry, JOTCSA. 2023;10(2):549–76.
3. Zangade S, A Review on Solvent-free Methods in Organic Synthesis, Current Organic Chemistry, 2019, 23, 2295-2318.
4. Mazimba O. Antimicrobial activities of heterocycles derived from thienylchalcones. Journal of King Saud University-Science. 2015;27(1):42–8.
5. üchter M, Ondruschka B, Bonrath W, Gum A. Microwave assisted synthesis–a critical technology overview. Green chemistry. 2004;6(3):128–41.
6. Khumraksa B, Phakhodee W, Pattarawarapan M. Ultrasound-assisted solventless synthesis of amines by in situ oxidation/reductive amination of benzyl halides. RSC Adv. 2014;4(39):20454–8.

STUDY OF THE CHEMICAL REACTIVITY OF PYRROLO-COUMARIN AND INDOLO-COUMARIN: A COMPUTATIONAL STUDY

Subhechha Sabud, Madhumita Bera, Souvik Pramanik and Jagannath Pal*

Department of Chemistry, Midnapore City College, Kuturia, Bhadutala, Paschim Medinipur, West Bengal 721129, India
*Corresponding author Email: jagannathpal24@gmail.com

Abstract

A derived from coumarin was studied using HF-method. Optimized geometries, the energy levels of the highest occupied molecular orbital and the lowest unoccupied molecular orbital, and ultraviolet-visible spectra were obtained using theoretical calculations, and they were also compared with experimental parameters. The representation of an excited state in terms of the natural transition orbitals was performed. Chemical reactivity parameters were calculated and correlated with the biological activity. A new proposal was obtained to design new molecular systems and to predict their potential use biologically active molecule.

Keywords: Coumarin, Hartree Fock, HOMO-LUMO study, Anticancer activity, ESP.

Introduction:

Coumarin is an aromatic compound with formula $C_9H_6O_2$. It can be prepared by the Perkin reaction between salicylaldehyde and acetic anhydride. Coumarin is found in many plants serve as chemical defense. In present day coumarin have a various range of pharmacological and excellent optical properties. It can used in optoelectronics, solar cells, laser, nonlinear optics and dye industries because coumarin have various properties that is solid state emission, large stocks shift, high emission yield etc. It can also use in anti-inflammatory, anti-tuberculosis, anti-HIV, anti-fungal, anti-rubulin, anti-coagulant, and antioxidant activity. Coumarin have an important role in the treatment of prostate, cancer, renal cell, carcinoma and leukemia. Again, Benzothiazole pharmacophore is known anticonvulsant, anti-inflammatory, antitumor, antimicrobial activities. Some of the coumarin with other heterocycles that is benzothiazole, antipyrine etc.exhibits antimicrobial, anticancer and antiberculosis activity. A fusion of pyrrole or indole to the different sites of the coumarin ring results in diverse molecular structures. There are two possible sites for the fusion of coumarin with pyrrole or indole ring producing pyrrolo[3,4-b]coumarin, indolo[3,4-b]coumarin derivatives. The pyrrolo[3,4-b]coumarin or chromeno[3,4-b]pyrrol-4(3H)-one

derivatives are one of the well-known natural marine alkaloids and synthetic compounds having an appreciable biological significance. Pyrrolocoumarins showed diverse biological activities including multidrug resistance (MDR) reversal, antitumor, and antiretroviral activities. They were also introduced as potent DYRK1A inhibitors.

2. Computational methodology

To investigate the biological activity of Coumarin and the Coumarin derivatives, are theoretical studies has been carried out. Ground state geometry optimizations were performed in gas phase using HF method. Frontier-Molecular orbital (HOMO & LUMO) calculations were performed in gas phase using the same method. The def2-SVP basis set was used for all the calculations. All calculation has been explored using ORCA software package. HOMO-LUMO was visualized using Avogadro Program.

3. Results and discussion

3.1 Molecular Geometry

The impact of the geometric structure on the electronic properties manifests itself through the bond length and bond angle across the compound backbone, the most relevant structural parameters of title compounds were determined by HF calculation using def2-SVP as basis sets. Using information obtained as a guide, molecular descriptors calculated using quantum mechanical methods enable determination of molecular quantities characterizing reactivity, shape and binding properties of molecules. The atoms numbering of molecule used in this paper is reported in Fig.1.

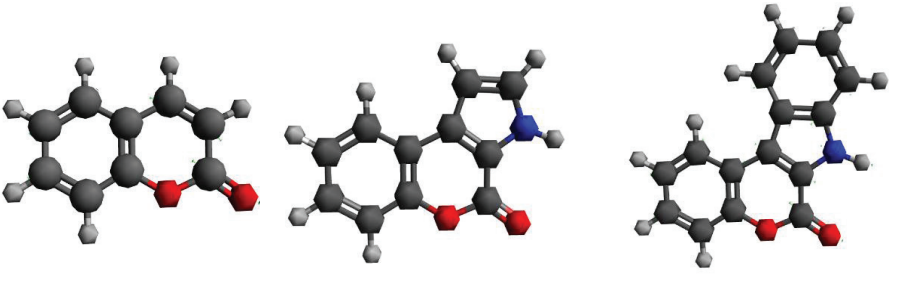

Coumarin **Pyrrolo[3,4-b]Coumarin** **Chromeno[3,4-b]indol 6(7H)-one**

Fig.1. Optimized geometric structure of Coumarin, Pyrrolo[3,4 b]Coumarin and Chromeno[3,4-b]indol-6(7H)-one.

3.2 Molecular Electrostatic Potential (ESP) Map

Molecular electrostatic potential (ESP) at a point in the space around a molecule gives an indication of the net electrostatic effect produced at that point by the total charge distribution (electron + nuclei) of the molecule and correlates with dipole moments, electro negativity, partial charges and chemical reactivity of the molecule. It provides a visual method to understand the relative polarity of the molecule. The different values of the electrostatic potential represented by different colors; red color represents the region of the most negative electrostatic potential; blue color represents the regions of the most positive electrostatic potential and white color represents the region of zero potential. For all compounds MEP was calculated by HF at svp-def2 basis set and MEP surface are plotted in Fig.2.

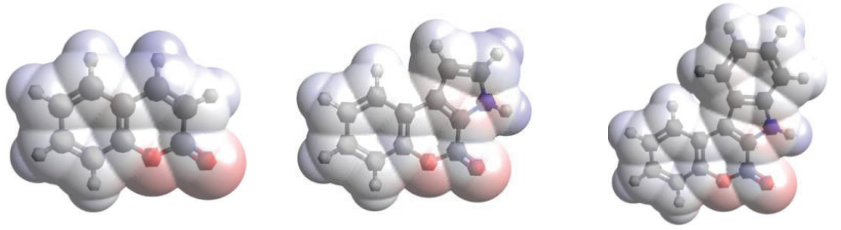

Coumarin Pyrrolo[3,4-b]Coumarin Chromeno[3,4-b]indol-6(7H)-one

Fig. 2. Visualization of Molecular Electrostatic Potential (ESP) for three selected compounds.

3.3 Thermochemistry

Throughout the following assumptions are being made: (1) The electronic state is orbitally non degenerate, (2) There are no thermally accessible electronically excited states, (3) Hindered rotations indicated by low frequency modes are not treated as such but are treated as vibrations and this may cause some error, (4) All equations used are the standard statistical mechanics equations for an ideal gas, (5) All vibrations are strictly harmonic.

Considering all the assumption and at 298.15 K temperature and 1.00 atm pressure thermochemistry parameter like total thermal energy (U), total enthalpy (H), total entropy (S), Gibbs free energy (G) by using HF method with svp-def2 basis set.

Table.1 Thermochemistry parameter data of entitled molecules

Parameter	coumarin	Pyrrolo[3,4-b]Coumarin	Chromeno[3,4-b]indol-6(7H)-o
Mass (AMU)	146.15	185.18	235.24
Total energy (au/mol)	-309689.25617	-391671.32441733	-487358.3913478
Total enthalpy (au/mol)	-309688.66368	-391670.73192555	-487357.7988560
Total entropy (au/mol)	25.25	27.78	31.22
Gibbs free energy (au/mol)	-309713.91576	-391698.51647095	-487389.0201875

3.4 Reactivity descriptors

Frontier Molecular Orbitals

The frontier molecular orbital determines the way in which the molecule interacts with other species. HOMO (highest occupied molecular orbital), which can be thought the outer most orbital containing electrons, tends to give these electrons such as an electron donor. On the other hand, LUMO (lowest unoccupied molecular orbital) can be thought the innermost orbital containing free places to accept electrons. Energy difference between HOMO and LUMO orbital is called as energy gap that is an important stability for structure. A molecule with a small gap is more polarized and is known as soft molecule. The frontier orbital (HOMO, LUMO) of three entitled molecules with HF method is plotted in Fig. 3.Chromeno [3,4-b]indol-6(7H)-one is found to be more reactive than all the compounds. Moreover, compound Chromeno[3,4-b]indol 6(7H)-one has the smaller frontier orbital gap so, it is more polarizable and is associated with a high chemical reactivity, low kinetic stability and is also termed as soft molecule.

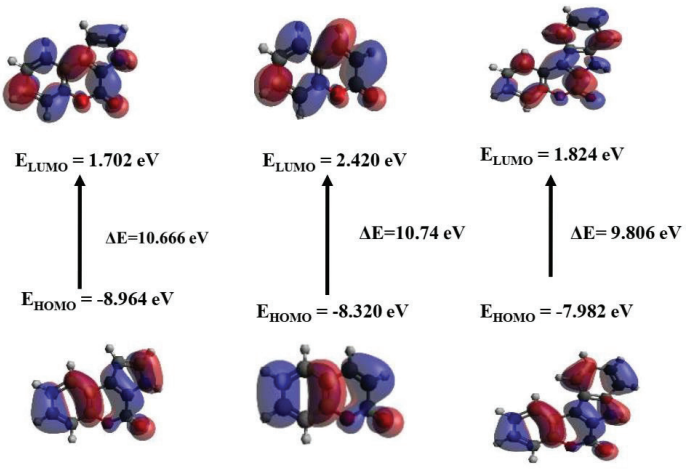

3.5 Global Reactivity Descriptors

The chemical reactivity of the molecular systems has been determined by the conceptual density functional theory. Electronegativity (χ), chemical potential (μ), global hardness (η), global softness (S) and electrophilicity index (ω) are global reactivity descriptors, highly successful in predicting global reactivity trends on the basis of Koopman's theorem, The global reactivity descriptor for the three titled molecules are listed in tables 1.

Table.2 Chemical Potential, Electronegativity, Global Hardness, Electrophilicity Index.

Compounds	μ (eV)	X (eV)	η (eV)	ω(eV)
Coumarin	-3.631	3.631	5.333	1.236
Pyrrolo[3,4-b]Coumarin	-2.95	2.95	5.37	0.81029
Chromeno[3,4-b]indol-6(7H)-one	-3.079	3.079	4.903	0.96678

4. Conclusions

A theoretical study of the stability and a reactivity was carried out at the Hartree Fock (HF) calculation level for the structure of Coumarin, Pyrrolo[3,4-b]Coumarin and Chromeno[3,4-b]indol-6(7H)-one. Reactivity index derive from HF calculation have

been successfully applied in understanding of chemical reactivity. Global descriptors such as ionization energy (I), molecular hardness (η), electrophilicity (ω), frontier molecular orbital shapes and energy gaps (ΔE), local ionization energy and electrostatic potential energy surface were determined and used to identified the differences of the reactivity of heterocycles.

In general, calculated values of η, ω, ΔH-L lead to the conclusion that the order of hardness is as: Pyrrolo[3,4-b]Coumarin> Coumarin >Chromeno[3,4-b]indol-6(7H)-one. So, molecule Chromeno[3,4-b]indol-6(7H)-one is softer than among the molecules. The HOMO-LUMO energy gape order is as: Pyrrolo[3,4-b]Coumarin > Coumarin > Chromeno[3,4-b]indol-6(7H)-one. So, molecule Chromeno[3,4-b]indol-6(7H)-one is more reactive than among of the all molecules and it has low kinetic stability.

References

1. Alorta I, Perez JJ. Molecular polarization potential maps of the nucleic acid bases. Int. J. Quant. Chem. 1996;57(1):123-135.

2. Bakhtiari G., Moradi S., SoltanaliS., 2014. A novel method for the synthesis of coumarin laser dyes derived from 3-(1H-benzoimidazol-2-yl) coumarin-2-oneunder microwave irradiation. Chem. 7, 972–975.

3. Biswal, S., Sahoo, U., Sethy, S.,Kumar, H. K. S., & Banerjee, M. (2012).Indole: the molecule of diverse biological activities. Asian J. Pharm. Clin. Res, 5(1),1-6.

4. BogerD.L., SoenenD.R., BoyceC.W., HedrickM.P., JinQ., Total synthesis of Ningalin B utilizing a heterocyclic azadiene Diels-Alder reaction and discovery of a new class of potent multidrug resistant (MDR) reversal agents, J. Org. Chem. 65 (2000) 2479-2483.

5. Chen L., XuM.-H., *Adv. Synth*

PHENOXAZINONE SYNTHASE MIMICKING ACTIVITY OF TWO TETRANUCLEAR COPPER(II) COMPLEXES

Manisha Das,[*a] Debashis Ray[*b]

[a]*Department of Chemistry, Midnapore City College, Kuturiya, Bhadutala, 721129, India.*

[b]*Department of Chemistry, Indian Institute of Technology, Kharagpur 721302, India.*

[a]*Email: manishachem90@gmail.com*

Abstract

Two tetranuclear copper(II) complexes have been synthesized following room temperature reaction in solution of Schiff base HL1 with $Cu(ClO_4)_2 \cdot 6H_2O$ in presence of two different ancillary ligands. External addition of sodium trifluroacetate and sodium benzoate in the reaction mixture of HL1 and $Cu(ClO_4)_2 \cdot 6H_2O$ gave μ_4-oxido-bridged $\{Cu_4\}$ complexes $[Cu_4(\mu_4\text{-}O)(\mu\text{-}L1)_2(\mu_{1,3}\text{-}O_2CCF_3)_4]$ (**1**) and $[Cu_4(\mu_4\text{-}O)(\mu\text{-}L1)_2(\mu_{1,3}\text{-}O_2CC_6H_5)_4]\cdot H_2O$ (**2**). Their functional bio-mimetic behaviour for copper ion-bearing oxidase enzyme phenoxazinone synthase have been established on model substrate *o*-aminophenol (OAPH) in MeOH medium. Kinetic analysis of the oxidation reactions was followed spectrophotometrically, which confirmed the involvement of Michaelis–Menten reaction kinetics. The presence of two different ancillary carboxylate clips in **1** and **2** showed difference in the catalytic turnover numbers.

Keywords: Copper(II), Schiff base, Phenoxazinone synthase mimicking activity, Michaelis- Menten kinetics, Turn-over number, *o*-aminophenol.

Introduction

Copper ion based coordination compounds from Schiff base ligand support have been extensively employed in a variety of laboratory and industrial applications, such as organic transformations and catalysis.[1] In living system, copper(II) ion is known to play a pivotal role in many important applications. In addition, copper ion based complexes have been widely distributed as the functional sites of various metal ion dependent enzymatic transformations like catechol and galactose oxidase, phenoxazinone synthase, superoxide dismutase, lysine oxidase, N_2O reductase activity.[2] Enormous efforts have been made by renowned research groups to mimic structural and functional sites of copper dependent enzymes aiming to develop better catalysts by tuning the electronic and geometric factors associated with the surrounding ligands.[3]

Catalytic oxidative coupling from 2-aminophenol (2-AP) to 2-amino-3H-phenoxazine-3-one (2-APX) by copper(II) based coordination compounds

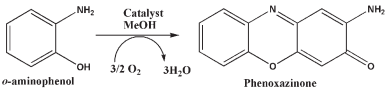

Scheme 1. Catalytic oxidation of *o*-aminophenol

has drawn considerable attention for its important mechanistic insights in the course of oxidative catalysis.[4] It has been experimentally observed that a naturally occurring antineoplastic agent, actinomycin D behaves as an inhibitor towards the preparation of DNA-directed RNA. Actinomycin D is related to questiomycin A, which is familiar as 2-Amino-3H-phenoxazine-3-one.[5] This species is used clinically for the treatment of certain types of cancer.[6] It is well observed that in the final step of the biosynthesis of actinomycin D, the enzyme phenoxazinone synthase catalyzes the oxidative coupling of 2-aminophenol to the phenoxazinone chromophore.[7] On account of the significance of the oxidative catalysis, the present work is based on the phenoxazinone synthase mimicking activity of two of our own μ_4-oxido-bridged $\{Cu_4\}$ complexes toward catalytic oxidative coupling of 2-aminophenol in air.

2. Experimental

2.1. Reagents and Materials

The chemicals used were obtained from the following sources: trifluoroacetic acid from SRL; sodium acetate from SD Finechem; sodium benzoate, copper hydroxide carbonate, triethylamine from Merck, India, allyl amine from Alfa Aesar and *o*-aminmophenol from SRL. $Cu(ClO_4)_2 \cdot 6H_2O$, sodium trifluoroacetate and 4-methyl-2,6-diformylphenol was prepared using literature reported procedure.[8] All the chemicals and solvents used in this work were of reagent grade and used as received without further purification.

2.2. Synthesis

2.2.1. Ligand HL1 [2,6-bis(allylimino)methyl)-4-methylphenol]

The ligand used in this work was prepared from a Schiff base condensation reaction involving allyl amine (1.05 g, 10mmol) and 4-methyl-2,6-diformylphenol (0.820 g, 5mmol) (3.5 g, 23.9mmol), in MeOH in 78% yield, as reported earlier.[8]

2.2.2. Synthesis of Complexes

$[Cu_4(\mu_4\text{-}O)(\mu\text{-}L1)_2(\mu_{1,3}\text{–}O_2CCF_3)_4]$ (1) and $[Cu_4(\mu_4\text{-}O)(\mu\text{-}L1)_2(\mu_{1,3}\text{–}O_2CC_6H_5)_4]\cdot H_2O$ (2)

Complexes **1** and **2** were synthesized by reacting HL1 (approx. 0.242 g, 1mmol) with copper(II) perchlorate hexahydrate (0.74 g, 2mmol) in MeOH using sodium trifluoroacetate (0.274 g, 2 mmol) as an auxillary ligand for **1** and sodium benzoate (0.288 g, 2 mmol) for **2** as reported earlier by us.[8] Selected FTIR stretching frequencies: (KBr, cm^{-1},): 1688 (vs), 1636 (m), 1436 (m), 1195 (vs) for complex **1** and 3447 (br), 1624 (vs), 1611 (vs), 1458 (m), 1370 (vs) for complex **2**. UV-vis spectra [λ_{max}, nm (ε, $Lmol^{-1}cm^{-1}$)]: (MeOH solution) 666 (104), 372 (8100), 261 (45400) for **1** and 635 (184), 366 (16400), 259 (91100) for **2**.

2.2.3. Procedure for the oxidation of 2-amino phenol in air

In this kinetic investigation, 2 mL of a MeOH solution (1×10^{-5} M) of complex **1** and **2** was prepared in a quartz cell and treated with 100 eq of 2-amino phenol (OAPH) substrate solution (1×10^{-3} M). The reaction was then followed at 25 °C by UV-Vis spectral scan at 5 min intervals up to 1 h for both complexes **1** and **2**. The kinetic analysis for the oxidation process was analysed based on the Michaelis–Menten equation.

3. Results and Discussion

3.1. Salient structural features of $[Cu_4(\mu_4\text{-}O)(\mu\text{-}L1)_2(\mu_{1,3}\text{–}O_2CCF_3)_4]$ (1) and $[Cu_4(\mu_4\text{-}O)(\mu\text{-}L1)_2(\mu_{1,3}\text{–}O_2CC_6H_5)_4]\cdot H_2O$ (2)

Two μ_4-oxido bridged $\{Cu_4\}$ complexes were synthesized following a straight forward room temperature complexation reaction in the presence of two different carboxylate anions. In both the complexes **1** and **2**, the carboxylate functions as a linker between two dinuclear $\{Cu_2\}$ entity. Mode of connection of two dinuclear entity by carboxylate bridge are different in these two complexes. In case of complex **1**, one copper(II) ion of one dinuclear moiety is connected to both copper(II) ion of second dinuclear unit by two trifluroacetato anions, whereas in case of complex **2** one copper(II) ion of one dinuclear unit is connected to another copper(II) ion of second dinuclear unit by two benzoate anion. Four copper(II) ions are connected by central μ_4-oxido anion adopting a near regular tetrahedral geometry. The other coordination sites are fulfilled by donors from the anion of HL1.

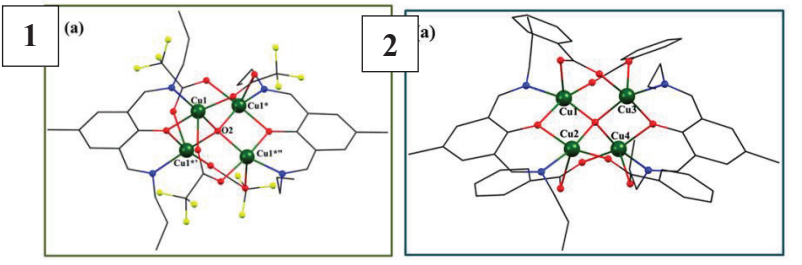

Figure 1. Structural view of **1** (left) and **2** (right) with partial atom numbering scheme and H atoms are omitted for clarity

3.2. Oxidation of 2-aminophenol and determination of the rate of formation of the phenoxazinone chromophore

Catalytic behaviour of complexes **1** and **2** was studied in MeOH solutions. The complexes **1** and **2** show absorbances at 372 and 366 nm. Upon addition of *o*-amino phenol, a new peak appeared at around 415 nm. The time dependent spectral scans for complexes **1** and **2** show gradual increase in the peak intensities at ~435 nm, characteristic for phenoxazinone formation, confirming the catalytic oxidation of *o*-aminophenol to 2-aminophenoxazine-3-one by O_2 of air. A blank experiment was performed without catalyst under identical conditions which does not show significant growth of the spectral band at ~435 nm. The time dependent spectral profile for a

period of ~1 hours in methanolic medium of complexes **1** and **2** is shown in Figure 2. The growth of phenoxazinone species was monitored at 435 nm as a function of time (Figure 2). The plot of rate constants versus concentration of the substrate displays the saturation kinetics (Figure 3) where Michaelis–Menten equation looks to be appropriate.

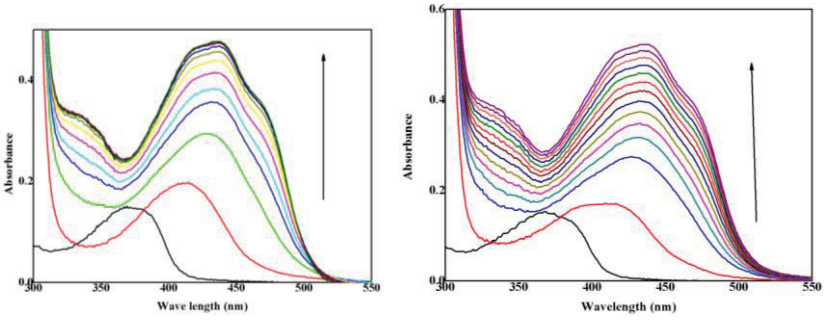

Figure 2. Increase of absorption spectra after addition of 100 equivalent of 2-aminophenol to a solution containing complex **1** (left) and **2** (right) (1×10^{-5} mol L^{-1}) in methanol. The spectra were recorded upto 1 h.

The Michaelis–Menten equation is

$$V = \frac{V_{max}[S]}{K_M + [S]}$$

where, V is the reaction velocity (the reaction rate), K_M is the Michaelis–Menten constant, V_{max} is the maximum reaction velocity, and $[S]$ is the substrate concentration.

The values of kinetics parameters were determined from Michaelis-Menten approach of enzymatic kinetics.

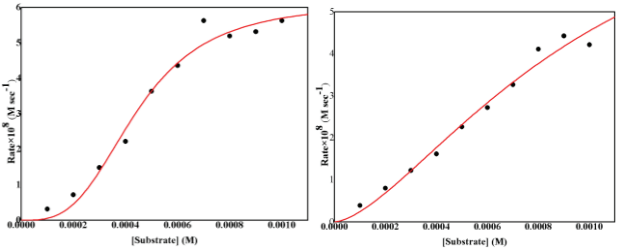

Figure 3. Dependence of the reaction rates on the substrate concentration for the oxidation of *o*-aminophenol catalyzed by complexes **1**–**2** in MeOH

Table 1. Kinetic parameters for the oxidation of 2-AP by **1** and **2** in MeOH

Complex	V_{max} (10^{-8} M S^{-1})	K_M (10^{-4} M)	k_{cat} (h^{-1})	k_{cat}/K_M (10^3 M^{-1} h^{-1})
1	6.1318	4.4306	22.0746	50

2	8.9871	9.8418	32.3537	33

4. Conclusion

Two synthesized tetranuclear copper(II) complex having different bridging connectivity by trifluroacetate and benzoate anion were used as a catalyst to study the oxidation reaction of model substrate 2-amino phenol. Both the complexes are active catalyst for oxidatative coupling of *o*-aminophenol to phenoxazinone. However, it was observed that the reactivity of complex **1** is higher than **2**. As observed in previous literature, the complex in solution exist as a dinuclear entity, and this dinuclear entity is responsible for the catalytic activity. The transformation to such entities facilitate the coordination of substrate to one of the copper(II) centre and thus have influence on catalytic efficiency. However, attachment of two different carboxylate moieties reflects the difference in their activity.

5. References

1. Smirnov AS, Martins LM, Nikolaev DN, Manzhos RA, Gurzhiy VV, Krivenko AG, Nikolaenko KO, Belyakov AV, Garabadzhiu AV, Davidovich PB. Structure and catalytic properties of novel copper isatin Schiff base complexes. New Journal of Chemistry. 2019;43(1):188-98.

2. Garai M, Dey D, Yadav HR, Choudhury AR, Maji M, Biswas B. Catalytic fate of two copper complexes towards phenoxazinone synthase and catechol dioxygenase activity. Chemistry Select. 2017 Dec 1;2(34):11040-7.

3. Mahapatra P, Ghosh S, Giri S, Rane V, Kadam R, Drew MG, Ghosh A. Subtle structural changes in ($Cu^{II}L$) $2Mn^{II}$ complexes to induce heterometallic cooperative catalytic oxidase activities on phenolic substrates (H_2L= Salen type unsymmetrical schiff base). Inorganic Chemistry. 2017 May 1;56(9):5105-21.

4. Jana NC, Patra M, Brandão P, Panja A. Biomimetic catalytic activity and structural diversity of cobalt complexes with N_3O-donor Schiff base ligand. Inorganica Chimica Acta. 2019;490:163-72.

5. Jana NC, Patra M, Brandão P, Panja A. Biomimetic catalytic activity and structural diversity of cobalt complexes with N_3O-donor Schiff base ligand. Inorganica Chimica Acta. 2019 May 1;490:163-72.

6. Kaizer J, Csonka R, Speier G. TEMPO-initiated oxidation of 2-aminophenol to 2-aminophenoxazin-3-one. Journal of Molecular Catalysis A: Chemical. 2002 Mar 11;180(1-2):91-6.

7. Maurya MR, Sikarwar S, Joseph T, Halligudi SB. Bis (2-[α-hydroxyethyl] benzimidazolato) copper (II) anchored onto chloromethylated polystyrene for the

biomimetic oxidative coupling of 2-aminophenol to 2-aminophenoxazine-3-one. Journal of Molecular Catalysis A: Chemical. 2005 Jul 18;236(1-2):132-8.

8. Das M, Canaj AB, Bertolasi V, Murrie M, Ray D. Strategic synthesis of [Cu_2], [Cu_4] and [Cu_5] complexes: inhibition and triggering of ligand arm hydrolysis and self-aggregation by chosen ancillary bridges. Dalton Transactions. 2018;47(47):17160-76.

THEORETICAL STUDIES OF THE CHEMICAL REACTIVITY OF A SERIES OF COUMARIN DERIVATIVES

Madhumita Bera, Subhechha Sabud Nabin Ch Adak and Jagannath Pal*

Department of Chemistry, Midnapore City College, Kuturia, Bhadutala, Paschim Medinipur, West Bengal 721129, India

*Corresponding author Email: jagannathpal24@gmail.com

Abstract

The global descriptors of reactivity such as HOMO and LUMO energies, chemical hardness, electrophilicity, softness and dipole moment are theoretically determined for two coumarin molecules in this paper. The analysis of the determined descriptors allows us to classify the studied molecules according to their reactivities. Thus, compound M_2 is qualified to be the most reactive and the least stable with 10.379 eV as its gap energy ΔE_{gap}. It is as the same time the softest, the best electron donners, the most nucleophilic and the most polar molecule. The study of thermodynamic parameters shows that all the reactions of formation of studied coumarin derivatives are exothermic and spontaneous with more disorder.

Introduction:

Coumarins are heterocyclic compounds which possess crucial importance in life because they play an essential role in the metabolism of all leaving cells. Coumarins are substances coming from plants and they have considerable therapeutic importance. They can exhibit potent biological and pharmacodynamic properties such as photosensitizing, antibiotic, anticoagulant (antivitamin) and antihemorrhagic properties. The study of heterocyclic chemistry is a widespread and growing field of chemistry with applications in medicine, agriculture, photodiodes, cosmetologyand many other fields. Several heterocyclic derivatives containing sulphur and/or nitrogen atoms serve as a unique and versatile scaffold for the design of new drugs. Coumarins are well known for their multiple biological activities including anticancer, anti-HIV, antitumor and antioxidant. According to their biological activities' usefulness, they have been considered as a subject of special attention. Regarding the harmful side effects of existing treatments for pathologies such as cancer and AIDS, access to new

therapeutic molecules that are effective and free of adverse effects has become the backbone of chemists. Computational chemistry is therefore both an independent research area and a vital adjunct to experimental studies. Hartree-Fock method (HF) is recognized as a popular approach for calculating the structural and energetic characteristics of molecule. This popularity is due to the fact that it provides very precise information for the evaluation of molecular properties. The general objective of this study is to determine theoretically the chemical reactivity sites of coumarin and their derivatives by the HF method.

2. Computational methodology

All the calculations were performed by using the HF method and def2-SVP was used as basis set. The calculations were performed with Avogadro 1.2 software. The output files were visualized using the Avogadro View graphical interface. All the calculations were performed over the optimized molecules characterized by the minimum of energy. Besides, the state is indicated by the absence of imaginary frequencies. Figure 1 displays the structures of the studied molecules. Frontier molecular Orbital theory (FMO) is used to characterized the overall reactivity of a compound. This theory predicts the excitation properties of a molecule. Therefore, it constitutes quantum parameters for the determination of molecular reactivity.
The chemical potential **μ** measures the tendency of electron cloud to escape from the molecule. The reactivity parameter can be expressed as a function of ionization potential PI and the electronic affinity AE. It corresponds to the opposite of the electronegativity **χ** as defined by Pauling and Mulliken.

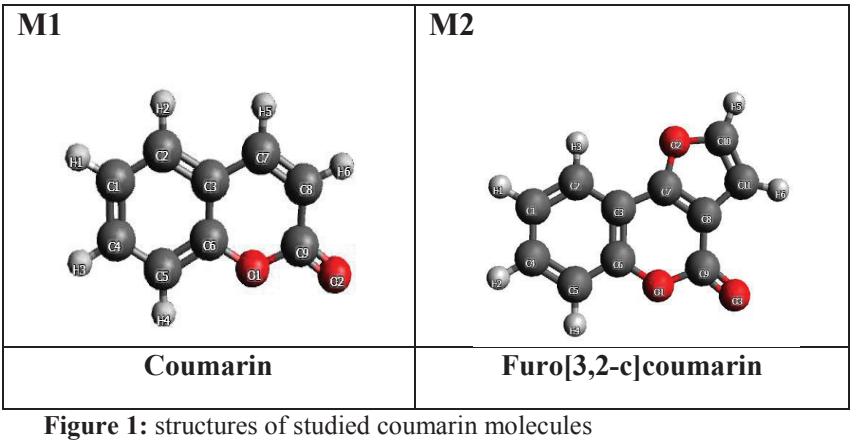

Figure 1: structures of studied coumarin molecules

3. Results and discussion

3.1. Thermodynamic descriptors

The thermodynamic parameters that were determined in this study are standard enthalpy of formation, standard free enthalpy of formation and standard entropy of formation. All values are summarized in Table 1.

Table1: The standard thermodynamic parameters of formation of studied compounds.

Molecules	$\Delta_f H^0_{298.15}$ (kcal/mol)	$\Delta_f G^0_{298.15}$(kcal/mol)	$\Delta_f S^0_{298.15}$(kcal/ mol)
M1	309690.1437	-309715.3985	25.25
M2	-404100.6518	-404128.3031	27.65

It is noted that any variation in enthalpy and free enthalpy reflects respectively the thermicity of chemical reaction and the spontaneity with which a chemical reaction takes place. As far as entropy is concerned, it provides relative information on the level of disorder in each chemical system. All the calculated values of thermodynamic parameters such as formation of enthalpy and formation of free enthalpy are negative and formation of entropy is negative. The negative values of enthalpy and free enthalpy mean respectively that the reactions are exothermic and spontaneous under the required conditions for the study. Furthermore, compound M2 is discovered as the most spontaneous and exothermic molecule during the synthesis. Regarding the entropy its positive value is assumed to increase the disorder during the synthesis of the coumarin molecules. Thus, the formation of all studied compounds is spontaneous and exothermic. According to overmentioned statement, it can be assumed that all these compounds exist and are thermodynamically stable.

3.2. Global Reactivity Descriptor

Global reactivity parameters are necessary for the classification of compounds according to their chemical reactivity. These descriptors are calculated from HOMO (Highest Occupied Molecular Orbital) and LUMO (Lowest Unoccupied Molecular Orbital) energies and they are grouped in Table 2.

Table 2: Global reactivity descriptors from frontier molecular orbitals (FMOs).

Parameters	M1	M2
HOMO(eV)	-8.964	-8.495
LUMO(eV)	1.702	1.884
Energy gap (ΔE)	10.67	10.38
Ionization energy (IP)	8.964	8.495
Electron affinity (AE)	-1.702	-1.884
Chemical Hardness(η)	5.333	5.190
Chemical Softness(S)	0.094	0.096
Chemical potential(μ)	-3.631	-3.306

Electronegativity(χ)	3.631	3.306
Electrophilicity index(ω)	1.236	1.053
Nucleophilicity index (N)	0.809	0.950
Electron accepting power(ω+)	0.136	0.171
Electron donating power(ω-)	3.767	3.476

Table 2 shows that compound M2 has the smallest value of the gap energy (ΔE_{gap} = 10.379), which allows to qualify it as the most reactive and the least kinetically stable among all the studied molecules. Conversely, the M1 is the least reactive with the highest value of the energy gap (ΔE_{gap} = 10.666) thereby appearing as the most stable compound, i.e., the least reactive molecule. The analysis of the other global reactivity indices, such as global softness (S) reveals that compound M2 displays the highest value (S = 0.096 eV). It is therefore admitted as the softest studied molecule. In addition, the nucleophilic index value of M2 (N = 0.950) indicates that it is the most electrophilic molecule. Other parameters such as the solubility which is studied by the mean of the dipole moment of the two studied compounds was also considered. The highest value of the dipole moment belongs to the compound M2. Therefore, M2is assumed to be the most polar compound. At the end of this analysis, we retain that M2 is the most reactive, the least stable, the softest, the best electron donner, the most nucleophilic and the most polar compound.

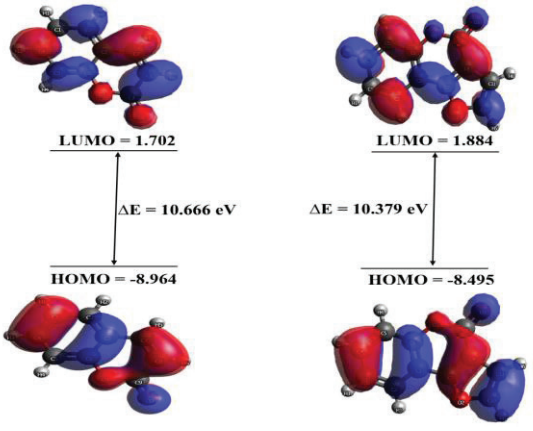

Figure 2: 3D HOMO – LUMO plot of M1 and M2

4. Conclusion

At the end of our study carried out by the HF method and def2-SVP was used as a basis set, we determined the most reactive molecule from the values of the global descriptors of chemical reactivity. The analysis of the results showed, on one hand that compound M2 is the most polar because, it has highest chemical reactivity and has both the lowest kinetic stability and the smallest energy gap of the studied

molecules. On the other hand, compound M1 is discovered as the least polar, with the lowest chemical reactivity and the highest kinetic stability. This work can help to understand the reactivity of coumarin derivatives and may be useful in the synthesis of new coumarin precursors.

4. References

1. Aihara, J. I., "Reduced HOMO-LUMO Gap as an Index of Kinetic Stability for

Polycyclic AromaticHydrocarbons," J. Phys. Chem. A, vol. 103, no. 37, pp. 7487–

7495, 1999.

2. Duquénois, P., "Coumarins et derives: Reparation dans le règne végétal biosynthesis,"Pharm.Biol.,vol. 7, no. 4, pp. 1107–1120, 1967.

3. Koopmans, T. "Über die Zuordnung von Wellenfunktionen und Eigenwerten zu den EinzelnenElektronen Eines Atoms," Physica, vol. 1, no. 1–6, pp.

A DISCUSSION ON THE BIOLOGICAL ACTIVITY OF COUMARIN, AZO DERIVATIVES, AND THE IMPORTANCE OF GREEN SYNTHESIS

Putul Karan and Avishek Ghosh*

Department of Chemistry, Midnapore City College, Kuturia, Bhadutala, Paschim Medinipur, West Bengal 721129, India

*Corresponding author Email: avishek.ghosh.mcc@gmail.com

Designing and then synthesis is a useful route to develop new kinds of molecules having different properties. In the field of drug discovery exploration of novel chemical components is an important area of special interest. Various naturally occurring products and biologically active molecules that are used extensively in medicinal chemistry have coumarin as key fragments. Coumarin and its derivatives, members of the flavonoid group, have numerous pharmacological applications; e.g. antioxidant, antimicrobial, anti-inflammatory, anti-carcinogenic, antinociceptive, hepatoprotective, antituberculosis, antithrombotic, antiviral, antidepressant, antihyperlipidemic and anticholinesterase properties [1]. To name some more, 4-methylumbelliferone acts as an antispasmodic and choleretic agent, 6-Methoxy-7-hydroxycoumarin shows good antioxidant, anti-inflammatory and antifungal properties, Coumarin based compound carbo chrome can be used in heart disease, anticoagulant activity is shown by different 4-Hydroxycoumarin derivatives. Coumarin itself and 7-hydroxycoumarin have both cytotoxic and cytostatic effects on different human cancer cell lines like gastric, colon carcinoma, hepatoma-derived cancer cell, hydroxy coumarin with nitro, methoxy, or hydroxy group show anti-proliferative effect in different cancer cell lines. Different recent literature reported potential biological activity of coumarin derivatives and their strong binding affinity towards DNA [2].

Recent literature studies show azo-bridged aromatic/heteroaromatic systems to be biologically active. They can act as antioxidants, antitumors, antidiabetics antimicrobials, and antiviral agents [3]. Various bacteria and fungi including Staphylococcus aureus, Streptococcus pyogenesetc, can be inhibited by 4-phenylazophenoxyacetic acid [4].

To protect the environment, using efficient, safe, and effective chemical methodologies for synthesizing desired bioactive molecules is the best way to prepare

new kinds of useful molecules. Using an aqueous medium during the synthesis is the best choice to protect the environment from harmful solvents. The literature review shows the syntheses of some aryl azo compounds linked to coumarin moiety in water. However, the biological activities of these compounds have not been explored. In view of the versatile application of coumarin analogues, herein we focus on the synthesis of some novel coumarin compounds and evaluate their biological activities.

Reference:

1. Manjunatha B, Bodke YD, Kumaraswamy HM, Pasha KM, Prashanth N. Synthesis, computational, hepatoprotective, antituberculosis and molecular docking studies of some coumarin derivatives. Journal of Molecular Structure. 2022 Apr 15;1254:132410.

2. Khoobi M, Emami S, Dehghan G, Foroumadi A, Ramazani A, Shafiee A. Synthesis and free radical scavenging activity of coumarin derivatives containing a 2-methylbenzothiazoline motif. Archiv der Pharmazie. 2011 Sep;344(9):588-94.

3. Prakash S, Somiya G, Elavarasan N, Subashini K, Kanaga S, Dhandapani R, Sivanandam M, Kumaradhas P, Thirunavukkarasu C, Sujatha V. Synthesis and characterization of novel bioactive azo compounds fused with benzothiazole and their versatile biological applications. Journal of Molecular Structure. 2021 Jan 15;1224:129016.

4. Jarrahpour AA, Motamedifar M, Pakshir K, Hadi N, Zarei M. Synthesis of novel azo Schiff bases and their antibacterial and antifungal activities. Molecules. 2004 Sep 30;9(10):815-24.

The conference on ***Current Trends and Future Extensions of Green Chemistry (CTFEGC-23)*** was organized by Department of Chemistry, Midnapore City College and sponsored by Council of Scientific & Industrial Research (CSIR), India. In this platform eminent scientists of India shared their immense knowledge, view-points on how negative impact of chemicals on the environment can be reduced and thereby bring sustainability in chemical production.

Dr. Avishek Ghosh is currently Assistant Professor, Coordinator, Department of Chemistry, Midnapore City College, Bhadutala. He completed his M.Sc in Chemistry from Vidyasagar University in 2011 and obtained his Ph.D from NIT Rourkela in 2019. He has authored several papers in peer-reviewed international journals. His research interest focused on synthetic organic chemistry.

Dr. Jagannath Pal is currently Assistant Professor, Department of Chemistry, Midnapore City College, Bhadutala. He completed his M.Sc in Chemistry from Vidyasagar University in 2011 and obtained his Ph.D from IIT Patna in 2021. He has authored several papers in peer-reviewed international journals. His research interest focused on computational chemistry.

Dr. Manisha Das is currently Assistant Professor, Department of Chemistry, Midnapore City College, Bhadutala. She earned her M.Sc in Chemistry from Vidyasagar University in 2012 and obtained her Ph.D from IIT Kharagpur in 2019. After that she joined IACS Kolkata, as a postdoctoral fellow under SERB-NPDF scheme (2020-2022). She has authored several papers in peer-reviewed international journals. Her research interest focused on synthetic inorganic chemistry.

Dr. Prankrishna Manna is currently Assistant Professor, Department of Chemistry, Midnapore City College, Bhadutala. He completed his M.Sc in Chemistry from Vidyasagar University in 2009 and obtained his Ph.D from Jadavpur University in 2015. He has authored several papers in peer-reviewed international journals. His research interest focused on synthetic coordination chemistry.

Co-Published by

Midnapore City College
West Bengal, India

Levant Books
India

ISBN : 978-93-91741-51-8

₹ 1495.00